Anal Bioanal Chem (2016) 408:1783–1803
DOI 10.1007/s00216-015-8953-2

REVIEW

Recent advances in biosensing using magnetic glyconanoparticles

Raluca M. Fratila[1,2] · **María Moros**[1] · **Jesús M. de la Fuente**[3,4]

Received: 15 June 2015 / Revised: 28 July 2015 / Accepted: 31 July 2015 / Published online: 18 August 2015

Abstract In this critical review we discuss the most recent advances in the field of biosensing applications of magnetic glyconanoparticles. We first give an overview of the main synthetic routes to obtain magnetic-nanoparticle–carbohydrate conjugates and then we highlight their most promising applications for magnetic relaxation switching sensing, cell and pathogen detection, cell targeting and magnetic resonance imaging. We end with a critical perspective of the field, identifying the main challenges to be overcome, but also the areas where the most promising developments are likely to happen in the coming decades.

Keywords Magnetic glyconanoparticles · Magnetic relaxation switching · Biosensing · Carbohydrates · Nanotechnology

Published in the topical collection *Analytical Applications of Biomimetic Recognition Elements* with guest editors Maria C. Moreno-Bondi and Elena Benito-Peña.

Raluca M. Fratila and María Moros contributed equally to this work.

✉ Jesús M. de la Fuente
jmfuente@unizar.es

[1] Instituto de Nanociencia de Aragon, Universidad de Zaragoza, C/Mariano Esquillor s/n, 50018 Zaragoza, Spain

[2] Fundación ARAID, C/María de Luna 11, Edificio CEEI Aragón, 50018 Zaragoza, Spain

[3] ICMA, CSIC/Universidad de Zaragoza, C/Pedro Cerbuna 12, 50009 Zaragoza, Spain

[4] Institute of Nano Biomedicine and Engineering, Key Laboratory for Thin Film and Microfabrication Technology of the Ministry of Education, Research Institute of Translation Medicine, Shanghai Jiao Tong University, Dongchuan Road 800, 200240 Shanghai, China

Introduction

Carbohydrates and their conjugates with other biomolecules such as peptides, proteins and lipids (glycoconjugates) are fundamental for a multitude of biological processes. For instance, the carbohydrates present on the cell surface (glycocalyx) are involved in many recognition and inflammatory events, cell adhesion and cell differentiation processes [1], and most proteins present in human blood are glycosylated and play key roles in inflammation, immunological response, signal transduction and neuronal development [2]. Moreover, correct glycosylation is essential for the folding of proteins and for their biological activity. Abnormal protein glycosylation can be indicative of different diseases, such as cancer and hepatic and autoimmune diseases [3–7]. Consequently, a great deal of research is focused on the development of efficient early diagnostic tools based on glycoprotein detection and identification. Typically, isolation and identification of glycoproteins and their glycoforms are accomplished by time-consuming and expensive methods, which combine several techniques and require highly trained personnel, thus preventing their implementation in point-of-care analysis.

Lectins are non-enzymatic carbohydrate-binding proteins able to decipher the information encoded in monosaccharides and oligosaccharides because of their reversible and highly specific interactions with the carbohydrate residues present in glycoproteins, glycolipids and glycans. The study of lectin–glycoconjugate interactions not only can provide useful information regarding the mechanisms involved in carbohydrate–protein interactions, but can also be a useful diagnostic platform based on the detection and characterization of glycosylated analytes in biological samples. On the other hand, understanding of these interactions could also contribute to the development of more efficient diagnostic and therapeutic tools, as several infections caused by pathogens are mediated

by the interaction between pathogenic lectins and host cell surface glycans.

The main drawback in the study of carbohydrate–protein interactions is the low affinity of interactions involving sugars. Drawing inspiration from nature, which compensates the low affinity by a multivalent presentation of the carbohydrate ligands, glyconanotechnology offers the possibility to develop multivalent platforms for the study of biologically relevant carbohydrate interactions [8, 9]. The high surface-to-volume ratio of nanoparticles allows the introduction of a high number of carbohydrate ligands on their surface and excellent control over the ligand density; moreover, different ligands (carbohydrates, but also other types of biomolecules such as peptides, antibodies and oligonucleotides) can be attached simultaneously to create multifunctional glyconanoparticles of high complexity [1, 9].

Among the different nanoparticles, magnetic nanoparticles (MNPs) display unique size-dependent and composition-dependent magnetic properties that are not observed in the bulk material. These properties have allowed the use of MNPs for a plethora of biomedical applications, including contrast agents for magnetic resonance imaging (MRI) [10], magnetic hyperthermia therapy [11], drug delivery [12, 13], bioseparation [14] and biosensing [15, 16]. MNPs are particularly suited for biosensing purposes. The magnetic background of biological samples is inherently low, therefore allowing high selectivity and signal-to-noise ratios even in complex-sample scenarios. Moreover, MNPs can be used to preconcentrate the analyte before the detection step, thus enhancing the sensitivity of the measurement. Another advantage is the possibility to merge MNP technology with microfluidic platforms towards point-of-care diagnostic devices with significantly enhanced sensitivity, speed and efficiency.

In this critical review we discuss the last and more relevant contributions using MNPs conjugated with carbohydrates as specific biorecognition elements (glycoMNPs) for biosensing applications, including magnetic relaxation switching (MRS), cell and pathogen detection, cell targeting and MRI applications. We discuss the main synthetic routes to obtain glycoMNPs, and we provide a critical perspective of the field of magnetic biosensing, identifying the key challenges, as well as the areas where the most promising developments are likely to happen in the coming decades.

Preparation of glycoMNPs

The coating of MNPs with carbohydrates is accomplished by two main routes: *in situ during the synthesis* of the MNPs and in a *post-synthetic functionalization step*. One-pot, in situ procedures involve the synthesis of the MNPs in the presence of carbohydrates, resulting in ligand adsorption onto the surface of the MNPs. In post-synthetic methods, suitably functionalized carbohydrates are introduced on the surface of the MNPs by ligand exchange, covalent linking or non-covalent functionalization based on affinity interactions. Each functionalization strategy has advantages and drawbacks, and the conjugation protocol must be designed in a way that ensures an optimal ligand presentation on the surface of the nanoparticles. The control over the density and spatial presentation of carbohydrates on the surface of glycoMNPs is crucial for biosensing purposes, as well as for other bioapplications. On the one hand, if the ligand coverage is excessively high, steric hindrance can interfere with or even compromise recognition events [9, 17, 18]. On the other hand, a low density of carbohydrate ligands can promote unspecific interactions such as adsorption of proteins present in the sample to be analysed [19].

One-pot synthesis of glycoMNPs

Co-precipitation of Fe(II) and Fe(III) salts in the presence of sugar derivatives (Fig. 1) is the simplest procedure to obtain carbohydrate-coated MNPs. Horák et al. [20] reported the first synthesis of 2-nm D-mannose-coated iron oxide nanoparticles via a one-pot protocol in which D-mannose was directly added to a mixture of $FeCl_2$ and $FeCl_3$ in an alkaline medium. To obtain larger (6-nm) nanoparticles, magnetite nanoparticles obtained by co-precipitation of $FeCl_2$ and $FeCl_3$ were oxidized to maghemite and coated with D-mannose in a similar fashion. In both cases, D-mannose acts as a metal-coordinating ligand by chelating to the Fe(II) or Fe(III) ions through the OH group in the C-2 axial position. Carbohydrate stabilizers containing carboxyl groups can also be used to obtain stable glycoMNPs. Kekkonen et al. [21] synthesized magnetite nanoparticles coated with D-gluconic acid, lactobionic acid and Ficoll® (a sucrose-based polymer), showing that larger carbohydrate stabilizers such as Ficoll® produced nanoparticles with increased stability when compared with D-gluconic and lactobionic acid. Baccile et al. [22] compared two one-pot synthetic routes for the preparation of magnetite nanoparticles stabilized by sophorolipids (natural functional glycolipids composed of two glucose units linked to an oleic acid moiety). In the first procedure the co-precipitation of iron salts was done in the presence of the glycolipid (one step), whereas in the second procedure the carbohydrate was added to the reaction flask after the precipitation of the nanoparticles (two steps). Magnetite nanoparticles were obtained only in the two-step procedure, whereas the one-step procedure led to poorly ordered ferrihydrite nanoparticles, whose formation was attributed to the complexation of Fe(III) with the COOH groups of the glycolipid.

Although generally simple and scalable, these procedures suffer from a lack of control over the size, crystallinity and monodispersity of the nanoparticles. Moreover, the diversity

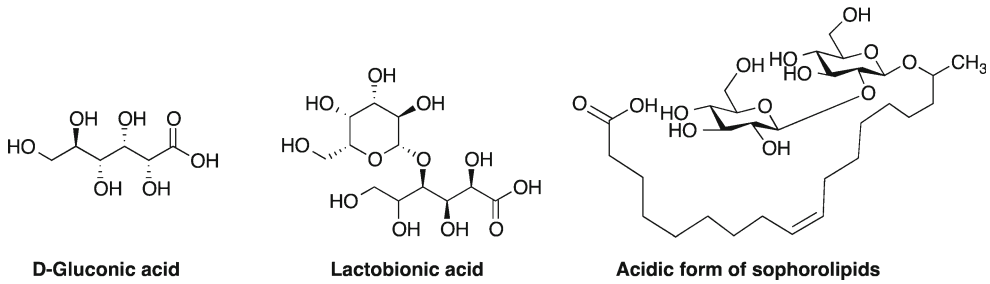

Fig. 1 Examples of carbohydrates used for direct synthesis of magnetic glyconanoparticles (glycoMNPs)

of carbohydrates that can be used to decorate the surface of the nanoparticles is rather limited.

Postsynthetic functionalization of MNPs with carbohydrates

Ligand exchange

Carbohydrates can be introduced on the surface of previously synthesized MNPs by a ligand exchange procedure (Fig. 2a). One of the commonest ligand exchange strategies exploits the affinity of phosphonate groups for the surface of iron oxide nanoparticles. Lartigue et al. [23] reported the first example of water-soluble rhamnose-coated iron oxide nanoparticles obtained by replacement of oleic acid and oleylamine ligands with phosphonate-functionalized rhamnose. Importantly, no leakage of rhamnose molecules from the surface of the nanoparticles was observed even on intense sonication at physiological pH, confirming the ligand attachment through strong iron–phosphonate bonds. Similarly, peracetylated mannose and ribose modified with phosphonate groups were used to illustrate the versatility of the approach [24]. Recently, Nativi et al. [25] designed a multivalent glycoconjugate nanoprobe based on iron oxide nanoparticles functionalized with a mimetic of the α-Tn antigen (a glycan antigen which is expressed in carcinoma-associated extracellular glycoproteins called mucins). The structures of the α-Tn antigen and its mimetic are depicted in Fig. 2b; the synthetic carbohydrate

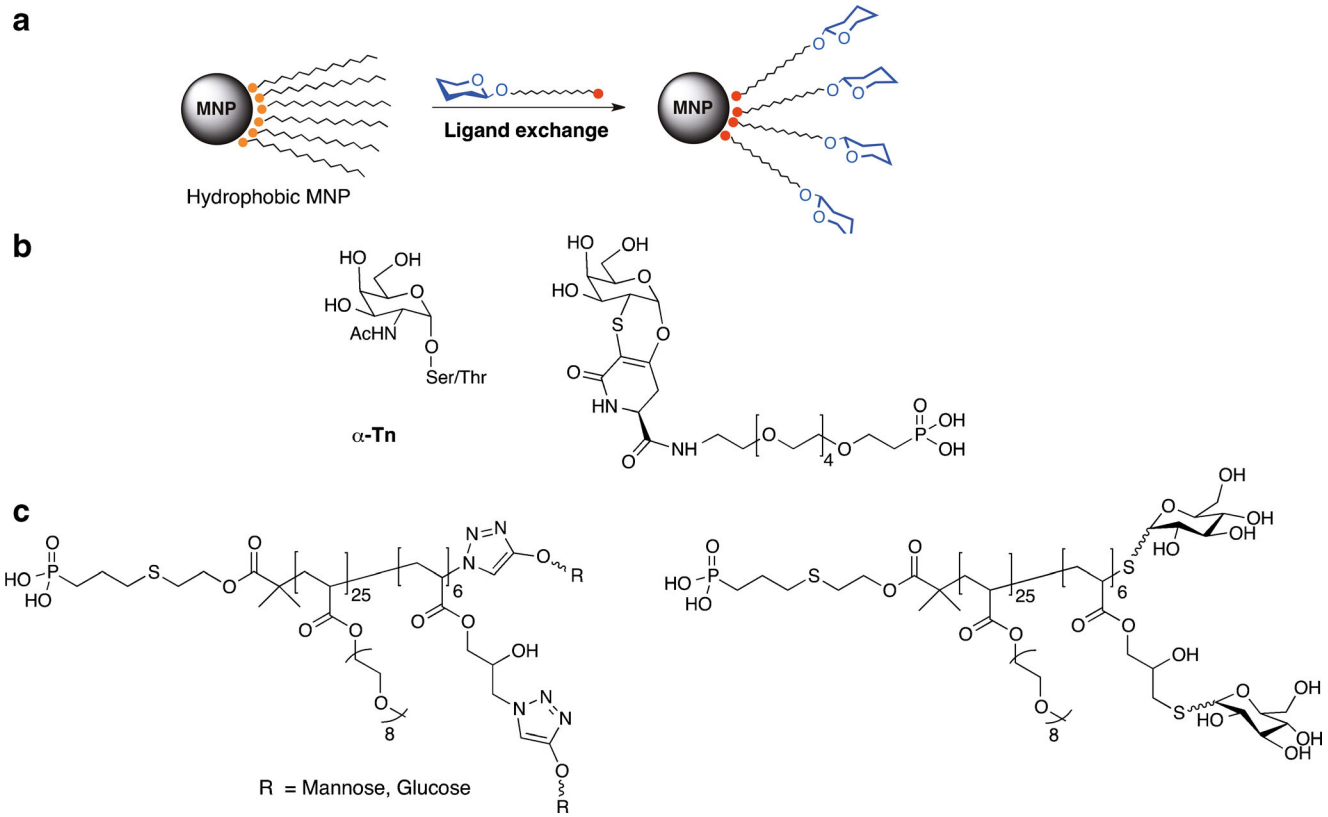

Fig. 2 **a** The ligand exchange reaction. **b** Structure of the α-Tn antigen and its mimetic used in the ligand exchange reaction. **c** Diblock polyethylene glycol glycopolymers bearing phosphonate groups. *MNP* magnetic nanoparticle. (**b** Adapted from [25] with permission of the Royal Society of Chemistry; **c** adapted from [26] with permission of the Royal Society of Chemistry)

maintains the key recognition elements of the native α-*O*-glycopeptide and incorporates a linker functionalized with terminal phosphonate groups for anchoring to the surface of MNPs. By inductively coupled plasma determination of the percentage of phosphorus in the functionalized MNPs, Nativi et al. estimated an average grafting density of 338 α-Tn mimetics per nanoparticle, which corresponds to 0.84 molecules per square nanometre. This indicated an almost complete coverage of the MNP surface with carbohydrates. Basuki et al. [26] reported the coating of iron oxide nanoparticles with diblock glycopolymers bearing phosphonic acid groups at one end and different sugars (α-D-mannose, α-D-glucose and β-D-glucose) at the other end (Fig. 2c). X-ray photoelectron spectroscopy data confirmed that the polymer attachment to the surface of the nanoparticles occurred through Fe–O–P bonds. All glycoconjugates displayed similar carbohydrate surface densities (about 225 sugar molecules per 10-nm MNP, as estimated from thermogravimetric analysis data). The glyconanoparticles showed good colloidal stability in water (more than 3 months), in *N*-(2-hydroxyethyl)piperazine-*N*′-ethanesulfonic acid buffer and in the presence of bovine serum albumin with no signs of aggregation.

The ligand exchange strategy can be applied also to hybrid MNPs, as reported by Gallo et al. [27], who prepared gold-coated metal-doped ferrite glyconanoparticles. Gold has a number of advantages as a coating material for MNPs as it protects the magnetic core against oxidation, increases biocompatibility and provides a platform for further functionalization, without affecting the magnetic properties of the core. In this work, superparamagnetic ferrite nanocrystals coated with gold were transformed into water-soluble ferrites (glycoferrites) by replacement of the hydrophobic oleic acid and oleylamine ligands with thiolated sugars by means of gold–thiol bonds. Different neoglycoconjugates of lactose, D-glucose and *N*-acetyl-D-glucosamine were used to obtain glycoferrites with 100 % sugar surface coverage. Importantly, this methodol allows tuning of the carbohydrate surface density. For example, glycoferrites with a 50 % carbohydrate density were obtained with a 1:1 mixture of neoglycoconjugate and a thiolated carboxylic acid in the ligand exchange step (Fig. 3). The carboxyl groups available on the surface of the glycoMNPs can be used as anchoring points for further functionalization to yield (immuno)fluorescent glycoMNPs [28–32].

Covalent functionalization with carbohydrates

One of the most straightforward and widely used covalent methods to construct MNP glycoconjugates is the classic amide bond formation mediated by carbodiimide coupling reagents such as water-soluble *N*-(3-dimethylaminopropyl)-*N*′-ethylcarbodiimide hydrochloride (EDC). The amide coupling can be done between MNPs bearing carboxyl groups and amino-functionalized carbohydrates or vice versa. However, a many examples reported in the literature use amino-functionalized MNPs and carboxylated sugars, most likely because of the relatively easy functionalization of MNPs with ligands containing amine groups. Our group has reported an optimized method for the synthesis of water-soluble magnetic iron oxide nanoparticles using an amphiphilic polymer, poly(maleic anhydride-*alt*-1-octadecene) [19]. Each anhydride unit yields two carboxylic acid groups on alkaline hydrolysis; this not only results in stabilization of MNPs in water over a broad pH range (4–11), but also provides a relatively high density of COOH groups for further functionalization. Under standard amide coupling conditions, COOH groups were reacted with NH_2 groups of 4-aminophenyl β-D-glucopyranoside and 4-aminophenyl β-D-galactopyranoside, respectively, to yield the corresponding MNP glyconconjugates (Fig. 4a) [19, 33]. A similar protocol was used to successfully functionalize gold-capped magnetite nanoparticles with glucose [34].

Park et al. [35] very recently reported the synthesis of fluorescent MNPs for the study of lectin-associated interactions in mammalian cells. Commercially available cobalt ferrite MNPs coated with a layer of silica containing rhodamine B isothiocyanate as a fluorescent probe were coupled to β-aminoethylated fucose-bearing oligosaccharides (Fig. 4b) with EDC. They estimated the glycan conjugation efficiency indirectly by labelling the remaining rhodamine B carboxyl groups with another fluorescent dye (Cy5), and concluded that approximately 80 % of the initial COOH groups were functionalized with the three saccharides.

As mentioned before, most covalent functionalization routes involving amide bond formation consist of the introduction of amine groups onto the surface of the MNPs and subsequent coupling with carbohydrates bearing carboxyl groups or other functional groups reactive towards amines. There are several protocols to decorate MNPs with amine groups. In one approach, the coating polymer (typically dextran used in the co-precipitation procedure to stabilize the MNPs) is cross-linked with epichlorohydrin, followed by treatment with ammonia. The sugar can be then linked to the amino-functionalized nanoparticles via classic amide bond formation or by use of *N*-hydroxysuccinimide-based bifunctional cross-linkers. Following this approach, Kouyoumdjian et al. [36] reported the synthesis of magnetite glyconanoparticles functionalized with approximately 100 sialic acid copies per nanoparticle for the detection of β-amyloid aggregates by MRI. Similarly, amino-functionalized silica MNPs were modified with carboxylic groups and decorated with Lewis X (Le^X) and sialyl Le^X (sLe^X) with use of the *N*-hydroxysuccinimide linker [37]. These glycoMNPs were used as a magnetic resonance contrast agent for imaging poststroke endothelial inflammation in mice. In an elegant example of rational glyconanoparticle design, van Kasteren et al. [38] used *S*-cyanomethyl as a "masked" functionality

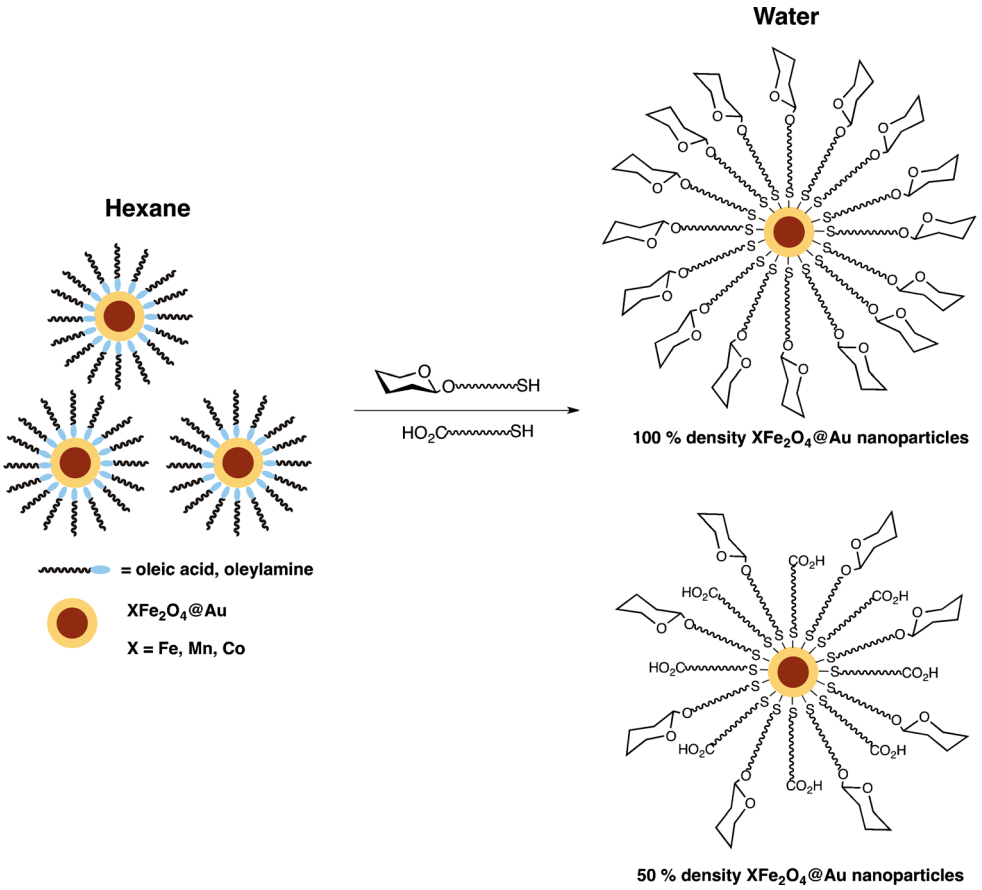

Fig. 3 Ligand exchange reaction for the preparation of glycoferrites with different carbohydrate surface coverage. (Adapted from [27] with permission of the Royal Society of Chemistry)

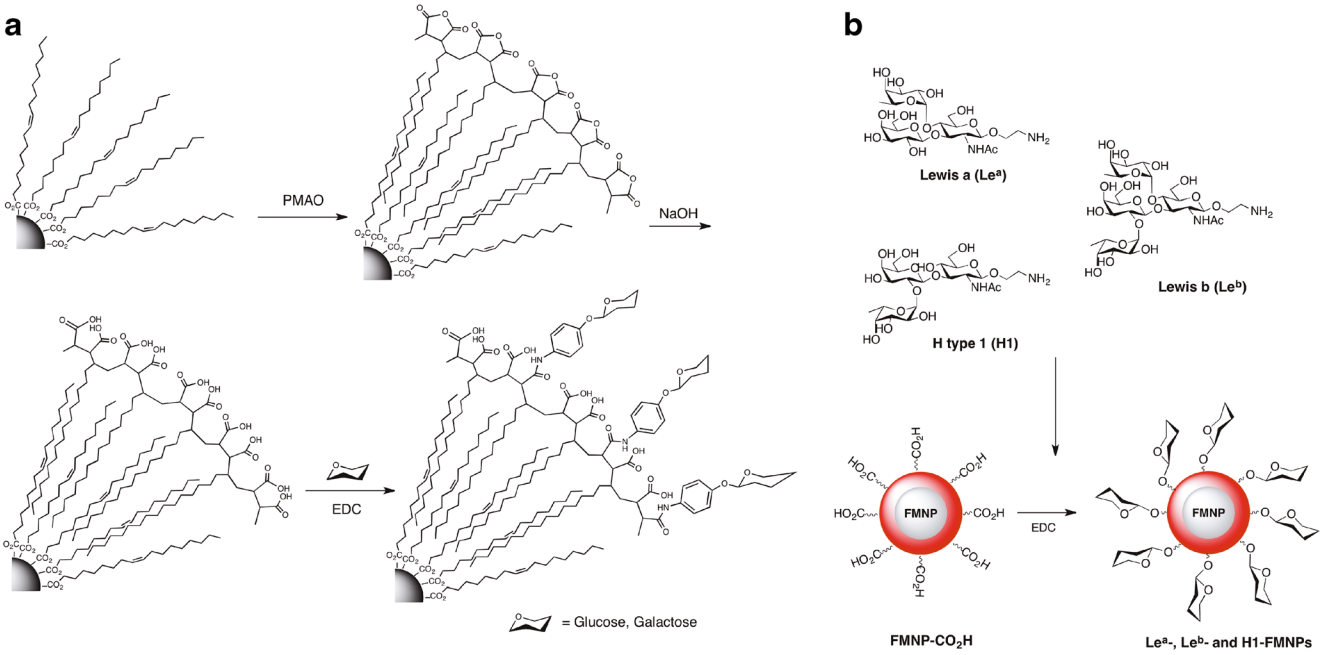

Fig. 4 **a** Functionalization of magnetic nanoparticles with amphiphilic poly(maleic anhydride-*alt*-1-octadecene) (*PMAO*) and covalent attachment of glucose. **b** Synthesis of fluorescent MNPs via covalent conjugation of amino-oligosaccharides to carboxylic acid groups present on the surface of the nanoparticles. *EDC* (3-dimethylaminopropyl)-*N*′-ethylcarbodiimide hydrochloride. (**a** Adapted from [19] with permission of the Royal Society of Chemistry; **b** Reprinted with permission from [35], copyright 2015 American Chemical Society)

through the synthesis of oligosaccharides of increasing complexity, from monosaccharides to tetrasaccharides. In the last step of the assembly of the glycoconjugates, the *S*-cyanomethyl moiety was activated to react with the amine groups present on the surface of amino-dextran-coated iron oxide nanoparticles. This procedure allowed the synthesis of glycoMNPs bearing multiple (10^5–10^7) copies of the tetrasaccharide sLe^X, whose interaction with selectins plays a key role in the first stages of the inflammatory cascade. The resulting glyconanoparticles were successfully used for in vivo imaging of brain lesions (for a critical discussion regarding magnetic resonance applications of the glycoMNPs described in [37–39], see "Imaging").

Alternatively, the surface of MNPs obtained by co-precipitation can be functionalized with aminosilane derivatives in a sol–gel process to yield amino-functionalized MNPs, which can be used as platforms to construct multifunctional glycoconjugates. For example, Lai et al. [39] synthesized HepG2 cancer cell targeting glycoMNPs incorporating a fluorescent dye (Cy3) and galactosyl derivatives of different valence (triantennary 1a, 1b and monoantennary 2a) and length (resulting in different ligand spatial presentation on the MNP surface). The ligands were attached to the amino-functionalized MNPs by bis(*N*-hydroxysuccinimide) chemistry (Fig. 5). Lai et al. demonstrated that the cellular uptake of the multifunctional glyconanoparticles by HepG2 cells was strongly influenced by the spatial orientation of the galactosyl ligands. The short triantennary conjugate 1a, in which the distance between galactose units is approximately 2.5 nm, corresponding to the spatial separation of the galactose-binding site of the lectin asialoglycoprotein receptor (AGSP-R; which mediates endocytotic uptake of glycoproteins), showed the most efficient internalization. Conversely, the trivalent derivative 1b, with a longer distance between galactose moieties (3.5 nm), showed a cellular uptake similar to that of the monovalent counterpart 2a. GlycoMNPs bearing glucose (2b) and sialic acid (2c) were synthesized following the same strategy and were used as negative controls to demonstrate that the cell internalization was governed by the specific recognition of galactose moieties by lectin.

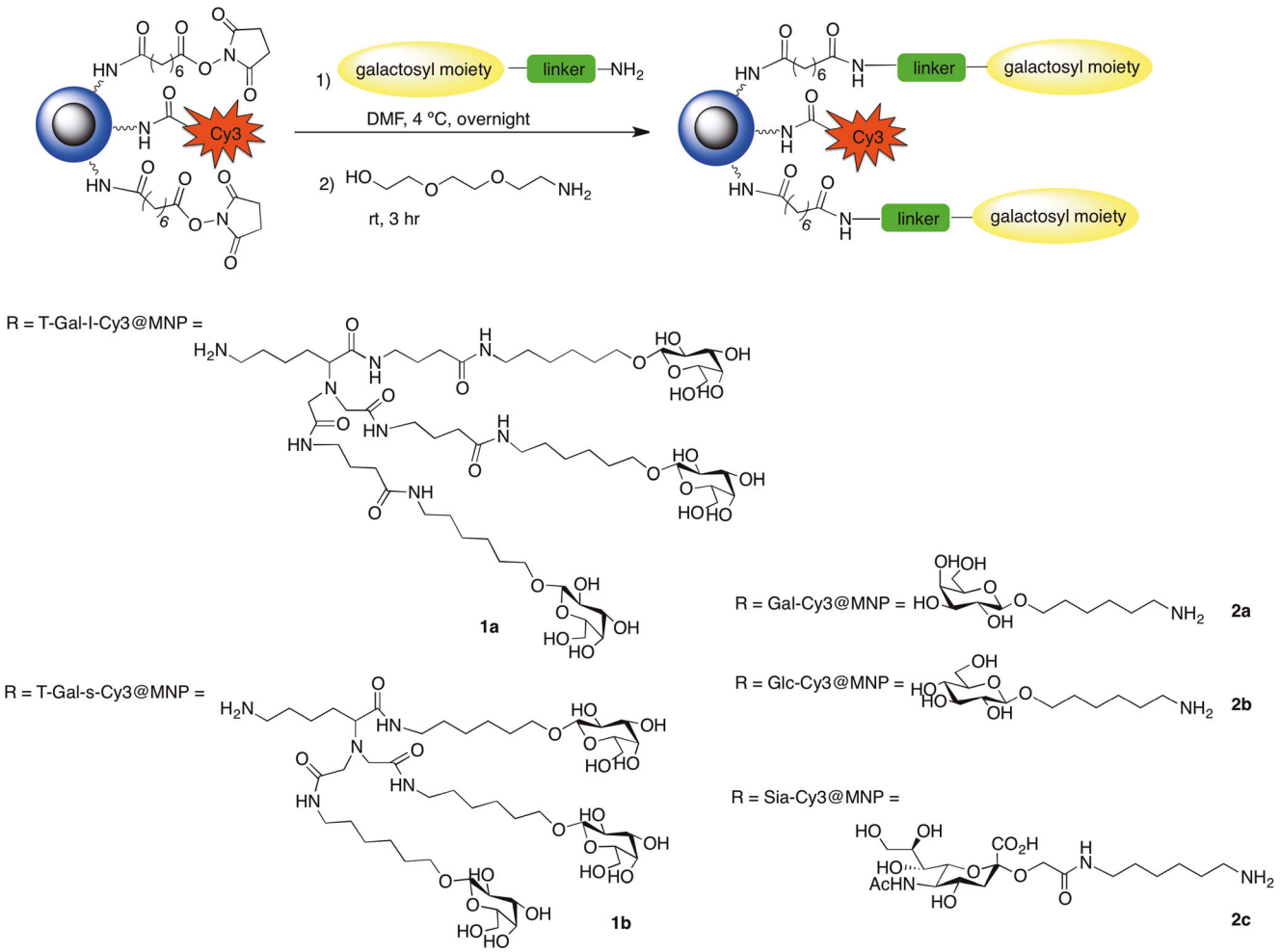

Fig. 5 Synthesis of monoantennary and triantennary fluorescent glycoMNPs. *DMF* dimethylformamide. (Adapted from [39] with permission of John Wiley & Sons)

Huang and co-workers [40, 41] reported the synthesis of glyconanoconjugates obtained by immobilization of carboxylic acid derivatives of different monosaccharides (glucose, galactose, mannose and sialic acid) on amine-functionalized MNPs. In this approach, amine groups were introduced onto the surface of magnetite nanoparticles by silanization with 3-aminopropyltriethoxysilane. However, the synthesis of the carboxylated sugars involved several reaction steps, including hydroxyl group protection and deprotection. From a synthetic economy point of view, conjugation methods compatible with the use of native, unprotected carbohydrates are desirable. To this end, the same authors explored the use of copper-catalyzed azide–alkyne "click" cycloaddition reaction of azido-functionalized MNPs with an unprotected *N*-acetylglucosamine derivative bearing an alkyne residue. The disappearance of the azide peak at 2095 cm^{-1} in the infrared spectra confirmed the successful immobilization of the alkynyl-*N*-acetylglucosamine on the MNPs.

As already mentioned, the density of carbohydrate ligands on the surface of glycoMNPs plays a key role in their stability and cellular uptake, as well as in recognition events [9]. Thus, control of functionalization is essential. Borase et al. [42] reported a combined strategy for the glycosylation of MNPs coated with 3-aminopropyltriethoxysilane, consisting of an alkyne polymer grafting followed by click chemistry using unprotected galactosyl azide (Fig. 6). The method yielded stable, water-soluble and monodisperse glycoMNPs with a high surface density of galactose ligands. This is the first example of a nanoglycoconjugate whose surface ligand coverage is not limited by the surface area of the nanoparticle. The polymer grafting introduces a high number of functional groups that can be further derivatized on demand; moreover, this grafting/click functionalization approach can be adapted to other nanoparticle systems with a similar silane-coated surface, regardless of their sizes.

The potential of click chemistry for developing glycoMNPs using unprotected sugars of higher structural complexity has also been demonstrated. For instance, Rouhanifard et al. [43] reported the synthesis of MNPs coated with poly(acrylic acid) and further functionalized with propargylamine. Click reaction with azido-Le^X was then done to yield multivalent Le^X-functionalized MNPs for detection and separation of dendritic cells (DCs; for more details, see "Pathogen and cell isolation" and Fig. 13, panel a).

Pfaff et al. [44] exploited the thiol–ene reaction (another standard click reaction widely used in bioorganic chemistry

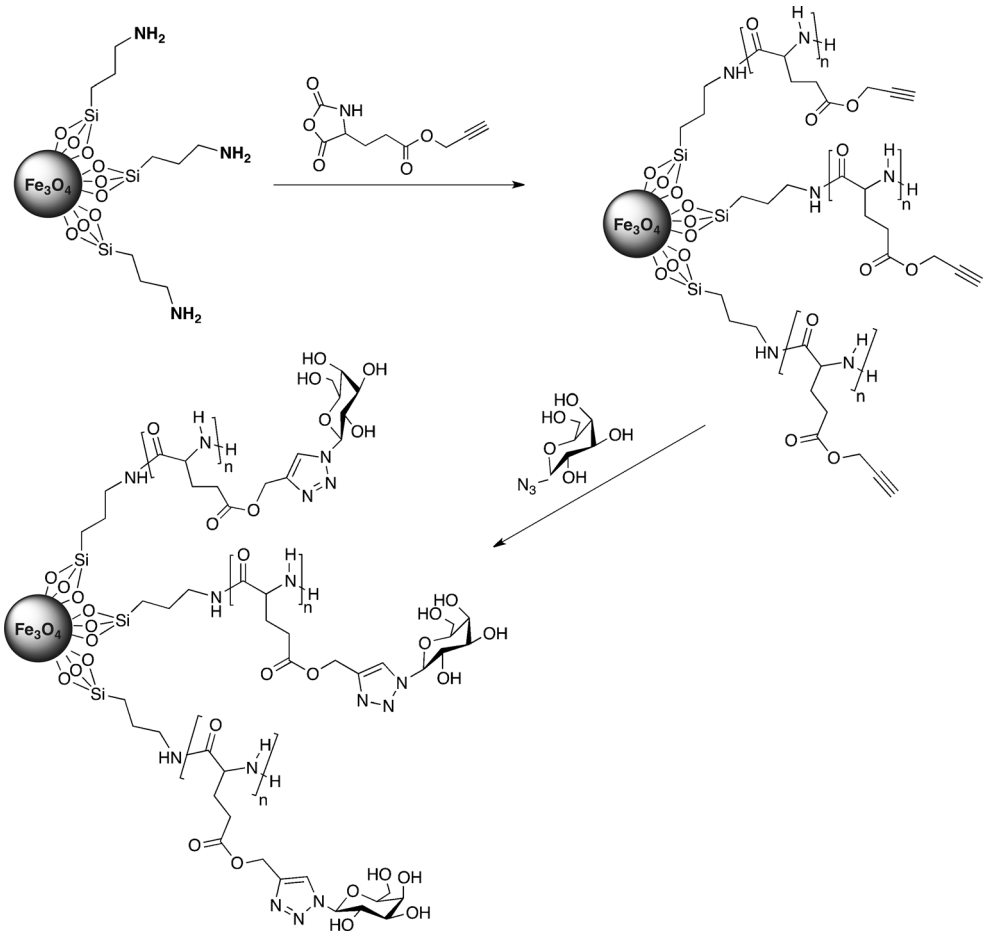

Fig. 6 Synthesis of glycopeptide-grafted MNPs. (Adapted from [42] with permission of John Wiley & Sons)

and materials science) between silica-encapsulated MNPs functionalized with methacrylate groups and thiolated fluorescent glycopolymers to construct multifunctional glycoMNPs for optical imaging. The main advantage of the thiol–ene reaction over the copper-catalyzed azide–alkyne cycloaddition strategy is the elimination of the copper catalyst, whose use can result in increased cytotoxicity even at low concentrations.

Another covalent functionalization strategy to introduce carbohydrates on the surface of MNPs relies on photoinitiated coupling of saccharide derivatives to MNPs bearing perfluorophenylazides (Fig. 7) [45, 46]. On irradiation with UV light, the azide group is transformed into a highly reactive nitrene functionality that can insert into CH and NH bonds. This approach has been used to functionalize MNPs of different compositions and geometries (spindle-type hematite and spherical magnetite nanoparticles) with monosaccharides and polysaccharides (D-mannose, D-maltoheptaose and β-cyclodextrin). A 1:1 mannose-to-perfluorophenylazide ratio was determined from thermogravimetric analysis data, indicating the efficient functionalization of all the perfluorophenylazide moieties present on the surface of 10-nm magnetite nanoparticles [45]. Although less exploited than other covalent functionalization strategies, this method is a convenient approach for the synthesis of glycoMNPs using native carbohydrates, therefore eliminating the need for their previous functionalization.

Non-covalent functionalization of MNPs with carbohydrates

Non-covalent methods to functionalize nanoparticles are based on the formation of affinity complexes relying on the extraordinarily high affinity of streptavidin for biotin, which leads to one of the strongest non-covalent interactions known in nature. Several magnetic-nanoparticle–streptavidin conjugates are commercially available, therefore simplifying the synthesis of glycoMNPs based on the biotin–streptavidin interaction. Despite these clear advantages, examples in which streptavidin–biotin interactions are used to construct glycoMNPs are scarce, with only two examples being found in the literature covering the last 5 years. Kulkarni et al. [47] used the non-covalent conjugation of monoantennary, biantennary and tetra-antennary carbohydrates functionalized with biotin (Fig. 8) to streptavidin-coated commercial magnetic beads (Invitrogen) to construct MRS sensors for the detection of toxins (see "Sensing through MRS"). In a similar fashion, Parera Pera et al. [48] synthesized galabiose–MNP conjugates by coupling biotinylated carbohydrates to 250-nm streptavidin-coated MNPs (purchased from Chemicell). These glycoconjugates were used for the specific detection of pathogenic bacteria (see "Pathogen and cell isolation").

GlycoMNPs for biosensing applications

Sensing through MRS

Throughout the years, many nanosystems bearing carbohydrates have been prepared as multivalent scaffolds for a variety of applications, such as sensing, imaging or cellular targeting [9, 49–51]. One of the major advantages of glycoMNPs over other systems is that they exhibit superparamagnetism [52], meaning that in the absence of a magnetic field and at room temperature, a spontaneous flip of magnetization occurs owing to thermal effects. The lack of remanent magnetization in the absence of a magnetic field is a major asset of these MNPs, as magnetic attraction between particles in solution is avoided, maintaining their stability and preventing aggregation. This feature can be exploited for detection and imaging applications, i.e. in the so-called magnetic

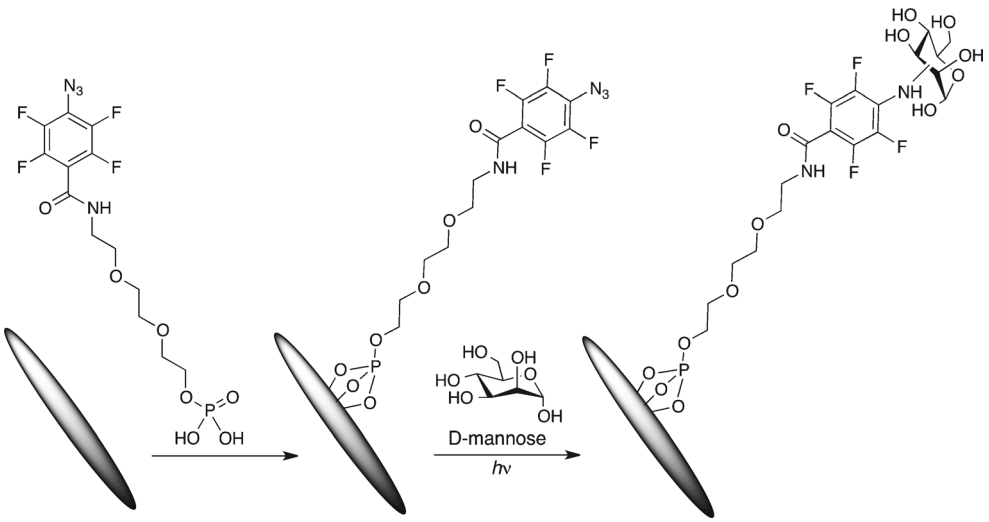

Fig. 7 Photoinitiated coupling of saccharides to MNPs. (Reprinted with permission from [45], copyright 2009 American Chemical Society)

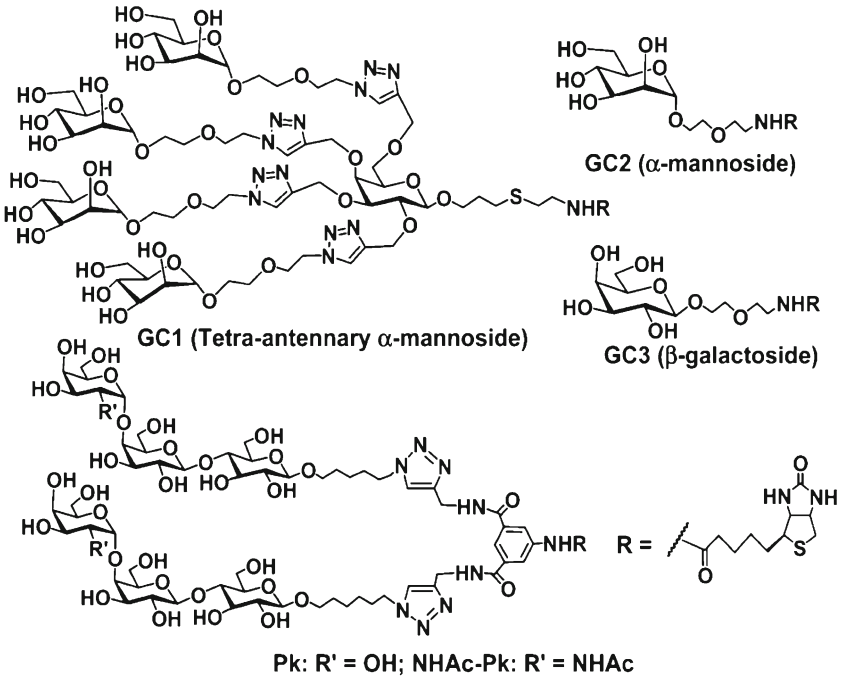

Fig. 8 Biotinylated carbohydrates for non-covalent attachment to streptavidin-coated MNPs. (Reprinted with permission from [47], copyright 2010 American Chemical Society)

relaxation switches, where the detection differences depend on the distinction between aggregated and non-aggregated states of the MNPs (see below).

When present in solution, MNPs induce local magnetic field inhomogeneities, which cause a dephasing (loss of phase coherence) of the proton spin precession. This ultimately leads to a shortening of the transverse (spin–spin) relaxation times (T2) of surrounding water protons [53]. These effects on T2 are normally used in MRI, as T2 shortening results in a decrease of the signal intensity, and therefore in the darkening of the image (negative contrast) [54]. More recently, and combined with the use of portable magnetic resonance systems, these changes have also been used for biosensing applications (MRS technology) [55]. This technology is based on the fact that dispersed MNPs have transverse spin–spin relaxation times (T2) different from those of clustered MNPs (Fig. 9).

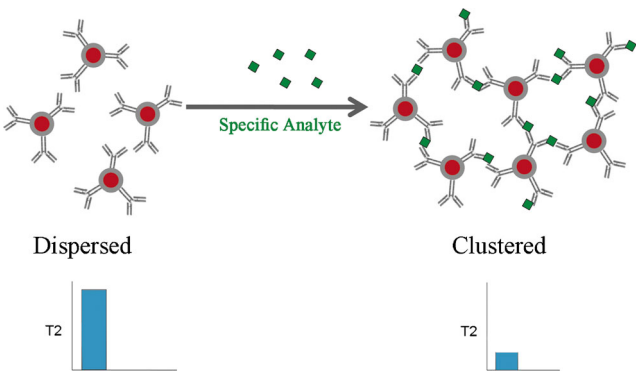

Fig. 9 Magnetic relaxation switching assay. Clustering of MNPs when a specific target is present induces a change in T2 that can be measured by NMR spectroscopy

To perform MRS assays, MNPs are generally multivalently functionalized with ligands that can bind simultaneously to a specific target molecule. When the target is present, particle aggregation occurs (Fig. 9). MNP multivalency plays a key role in the interaction of the ligand and the target, and it is therefore directly related to the sensitivity of the assay [56]. MNP aggregates can be dispersed again by different factors, such as temperature, enzyme cleavage or competitive binding analytes (relaxation switches) [57]. The resulting changes in T2 can be detected by nuclear magnetic resonance (NMR) spectroscopy. Unlike optical sensors, NMR spectroscopy uses radiofrequency radiation. This type of radiation can penetrate biological samples independently of their optical properties, and therefore assays can be performed in complex samples such as blood or milk [58]. In addition, biological samples exhibit low magnetic susceptibility, and therefore no magnetic background, and thus MNPs can be easily distinguished from the rest of the sample. Assays using MRS are non-destructive and fast, as they are performed in the entire sample volume and do not require washing steps. In contrast, the extent of MNPs clustering many times requires extensive optimization to achieve the maximum sensitivity, as it depends on the ratio of target molecules and MNPs [16].

In pioneering work, Sun et al. [59] developed glucose-functionalized MNPs by reacting amino cross-linked iron oxide nanoparticles with succinic anhydride, followed by incubation with EDC and 2-aminoglucose. Changes in T2 were recorded after addition of a fixed amount of concanavalin A (ConA), a lectin isolated from jack bean meal, which exhibits affinity for mannose and glucose-containing carbohydrates. ConA is a multimeric protein bearing four carbohydrate-

binding sites at pH 7; therefore, when it was placed in contact with the glycoMNPs, their agglutination occurred. To further demonstrate the specificity of the interaction, excess glucose was added. The free carbohydrate acted as a competitive inhibitor, binding to the ConA; on dispersion of the MNPs, the T2 values switched to the initial ones. Therefore, the MRS could be used to monitor analyte levels in a continuous way.

Similarly, we exploited this strategy using 8-nm MNPs coated with poly(maleic anhydride-*alt*-1-octadecene) [19]. EDC was used to functionalize the carboxylic groups present in the polymer with 4-aminophenyl β-D-galactopyranoside or glucopyranoside (see "Postsynthetic functionalization of MNPs with carbohydrates" for more details on the functionalization method). To perform the MRS assays, the stability of MNPs during the assay is of the utmost importance, to avoid unspecific aggregation of the MNPs when the ligand is not present. The adsorption of large proteins such as bovine serum albumin onto the surface of the glycoMNPs could be prevented even at a low density of glucose, indicating that carbohydrates could be used as an alternative to polyethylene glycol (PEG) derivatives for passivation of MNP surfaces. Adsorption of small and positive blood proteins (lysozyme) could be avoided at higher glucose-to-MNP ratios. Once we had tested the stability of both glycoMNPs, ConA was added, resulting in specific T2 changes only with glucose-functionalized MNPs but not with galactose-functionalized ones (Fig. 10a). The T2 values decreased as the ConA concentration increased, as bigger aggregates were formed, which was also demonstrated by our measuring the aggregate sizes by dynamic light scattering (Fig. 10b). Fitting the changes in T2 (ΔT2) values to the amount of added ConA allowed the affinity of the lectin–glycoMNP system to be studied, and a dissociation constant of 78 nM was obtained [60]. This value was similar to the value obtained with the same glycoMNPs and transient magnetic birefringence as the detection technique [60]. The apparent dissociation constant for this ConA–glycoMNP system is similar to those reported for other glycosystems where the carbohydrates are attached to the nanoparticles [61, 62], but is much lower than the value reported when the ligands are in solution (K_D on the order of micromolar) [63]. For this dissociation constant, cooperative interactions and accessibility to the carbohydrates play a fundamental role. Indeed, we demonstrated that apparent cooperativity existed (Hill coefficient greater than 1)—that is, the binding of one ConA molecule to a glycoMNP could favour the binding of the following one in a cooperative way.

Kulkarni et al. [47] reported the use of an MRS assay to detect in a sensitive way two isoforms of Shiga toxins. To set up the experimental conditions, they synthesized carbohydrates that were known to selectively bind different lectins: α-mannosides, which bind to ConA or *Galanthus nivalis* lectin, and β-galactoside to bind to *Ricinus communis* lectin (RCA120) and the plant toxin ricin. The carbohydrates were modified with biotin so that they could bind to micrometre-sized magnetic particles coupled with streptavidin. To test if the glycoMNPs could be used in MRS assays, they were incubated with the different lectins, and ΔT2 values were recorded with a 60-MHz benchtop NMR system. As expected, when MNPs bearing mannosides were incubated with ConA or *G. nivalis* lectin, aggregation occurred, although with different aggregation rates depending on the lectin used, and a change in T2 values was recorded. No differences in T2 values were observed when these MNPs were incubated with RCA120, indicating specificity. The ΔT2 values were greater for MNPs functionalized with tetra-antennary mannoside compared with those obtained for monoantennary mannoside,

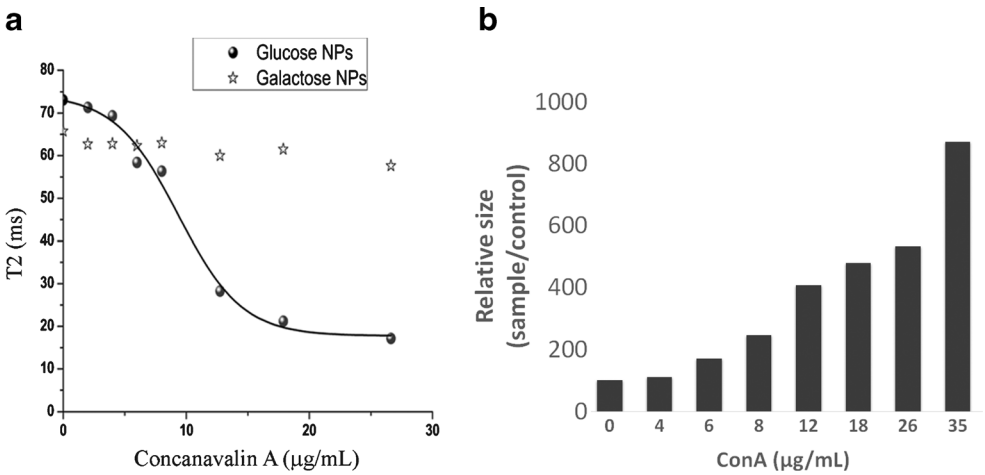

Fig. 10 **a** T2 values obtained after incubation of glucose- functionalized or galactose-functionalized MNPs with concanavalin A (ConA) for 5 min. Addition of increasing concentrations of ConA to glucose-functionalized MNPs resulted in a sigmoidal curve as a function of T2. Galactose-functionalized MNPs did not show any change in T2 values. **b** Relative size increase of the glucose-functionalized MNPs on addition of increasing amounts of ConA measured by dynamic light scattering. *NPs* nanoparticles. (Adapted from [19] with permission of the Royal Society of Chemistry)

even when the amount of attached molecules per MNP was smaller for the tetra-antennary mannoside. Similarly, β-galactoside-coated MNPs gave specific ΔT2 changes when they were incubated with RCA120. Plotting ΔT2 (%) against RCA120 concentrations allowed the limit of detection of the lectin to be determined, 0.62 nM. To further demonstrate the versatility and utility of this MRS assay with more complex samples, MNPs were functionalized with Pk trisaccharides or their N-acetylated analogues, which bind preferentially to Shiga toxin Isoform 1 and Shiga toxin isoform 2, respectively. Experiments were conducted using unpurified toxins from bacterial cultures to test the specificity of the system. As expected, Shiga toxin Isoform 1 bound only to Pk-coated MNPs, whereas Shiga toxin Isoform 2 bound only to N-acetylated Pk MNPs. Therefore, in 25 min it was possible to detect these closely related toxins in complex mixtures just by measurement of ΔT2. Shiga toxin isoform 2 was also detected in milk, juice, hamburger and stool samples. The limit of detection of Shiga toxin was 1 pg/mL in spiked stool samples, much lower than the sensitivity reported for commercial ELISA kits. Importantly, the test was performed in a single step, and no washing steps were required.

A similar assay was described by Cai et al. [64]. In this case, the MRS assay was designed to detect an acute-phase plasma glycoprotein, α_1-acid glycoprotein (AGP). To do so, dextran-coated MNPs were incubated with a fixed amount of ConA, and T2 changed during the first few minutes, but remained constant for at least 1 h during the measurements. Further addition of AGP caused the redispersion of these aggregated MNPs, and the ΔT2 values from the aggregated to the dispersed state were used to detect the amount of AGP present in the solution. The sensitivity obtained was 28.4 ng/mL, which is much lower than the normal concentration of AGP present in human plasma. Although the assay was validated as a proof of concept, to apply it to real serum samples other modifications should be made to ensure its specificity, as interferences with other glycoproteins present in the serum could occur.

A great example of the application of MRS with glycoMNPs was reported by El-Boubbou et al. [40]. Five kinds of carbohydrates (mannose, *N*-acetylglucosamine, galactose, fucose and sialic acid) were functionalized on 6-nm MNPs and used to detect and profile cancer cells. Nine types of cancer cells, together with a normal one, were incubated with the glycoMNPs, and the changes in T2 values were measured by MRI. Thirty samples could be measured at the same time, speeding up the whole process. By analysing the changes in T2 values for the five types of glycoMNPs through a statistical method, El-Boubbou et al. were able to establish specific molecular signatures for each cell line (Fig. 11a). Strikingly, on the basis of the magnetic resonance signatures, they were able to distinguish between cancer and normal cells (Fig. 11b), and even between closely related isogenic sublines of cancer cells (Fig. 11c).

Pathogen and cell isolation

One field where glycoMNPs have attracted great attention is pathogen detection. The adhesion of bacteria, before infection, is frequently mediated by bacterial proteins and tissue carbohydrates; therefore, these interactions could be used to develop bacterial detection tools [65]. Rapid detection and classification of bacteria is of the utmost importance, as classic culture methods are time-consuming. In this sense, MNPs have the unique advantage than the bacteria attached to the glycoMNPs can be separated from the unbound ones just with a magnet. Pioneering work of El-Boubbou et al. [66] and Hatch et al. [67] demonstrated that MNPs functionalized with glycoconjugates could be used to isolate and quantify *Escherichia coli*, reaching higher sensitivity and selectivity than the same MNPs functionalized with antibodies [67]. Since then, some other examples where glycoMNPs are used to detect bacteria can be found in the literature [68]. Parera Pera et al. [48] exploited this concept for the detection, for the first time, of a gram-positive pathogen, *Streptococcus suis*. They functionalized 250-nm MNPs with streptavidin, and later incubated them with biotin-linked monovalent or tetravalent galabiose. The resulting glycoMNPs were incubated for 1 h with different dilutions of *S. suis*, and after magnetic concentration, bound bacteria were detected by a luminescence assay. The detection limit was on the order of 10^4 bacteria per millilitre. Noticeably, this limit of detection was better for the monovalent galabiose than for the tetravalent one, owing to the different multivalent presentation of the glycans on the MNP surface.

Highly porous particles have also been used for *E. coli* removal [69]. This system was based on magnetic, porous, sugar-functionalized (MaPoS) PEG particles. The MaPoS particles were composed of a porous PEG hydrogel, functionalized with mannose and 8–15 nm MNPs, yielding microparticles with large surface areas. *E. coli* removal efficiency was around 70 % for bacteria-to-particle ratios below 30:1. MaPoS particles were more effective in removing *E. coli* than non-porous MNPs, as owing to their porosity and large surface area they were able to bind three to four times more bacteria.

More recently, Park et al. [35] have developed dual-modal fluorescent glycoMNPs able to recognize mammalian and pathogenic cell surface lectins. *Helicobacter pylori* is an infectious pathogen that causes chronic gastritis, in which the adherence of *H. pylori* to the gastric mucosa plays an important role. Among other molecules, the blood group antigen binding adhesin (BabA) is known to recognize Lewis b (Le^b) present in the gastric mucosa. To determine if glycoMNPs could be used to fluorescently detect *H. pylori*, cobalt ferrite MNPs coated with silica containing a fluorescent dye (rhodamine B) were functionalized with different types of oligosaccharides, Le^b and blood group antigen H type 1 (H1). The glycoMNPs were incubated with two *H. pylori* strains,

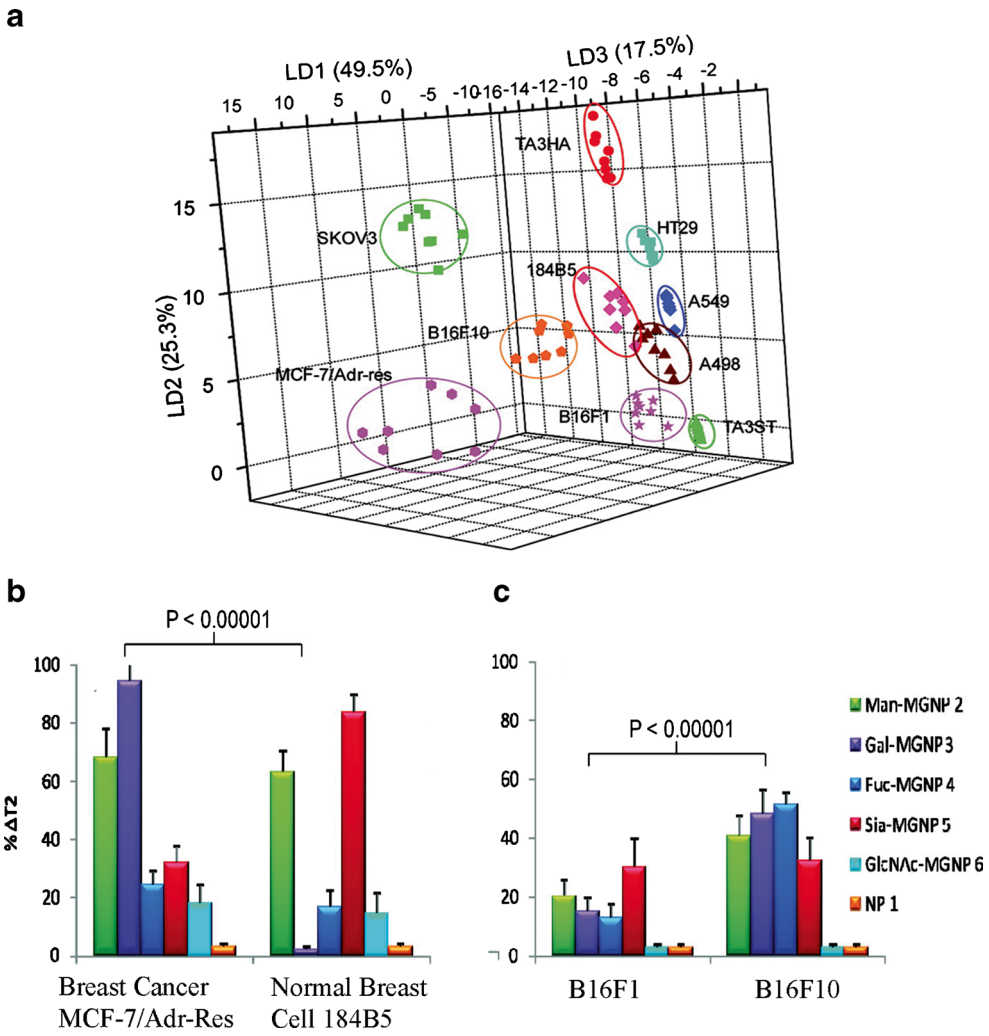

Fig. 11 **a** Statistical plot of ΔT2 patterns obtained with a glycoMNP array on binding with ten cell lines. Full differentiation of the ten cell lines was achieved. Percentage changes of the T2 relaxation time obtained on incubation of glycoMNPs or the control MNPs with **b** MCF-7/Adr-res breast cancer cells versus 184B5 normal breast cells and **c** B16F1 cells versus B16F10 ells. (Adapted with permission from [40], copyright 2010 American Chemical Society)

J99 (expressing BabA) and 26695 (not expressing BabA). After incubation for 1 h, confocal microscopy images revealed that Le^b-functionalized and H1-functionalized MNPs were able to recognize BabA expressed in the J99 strain, but none of them bound to the 26695 strain. These glycoMNPs were further incubated with human gastric carcinoma cells (AGS)

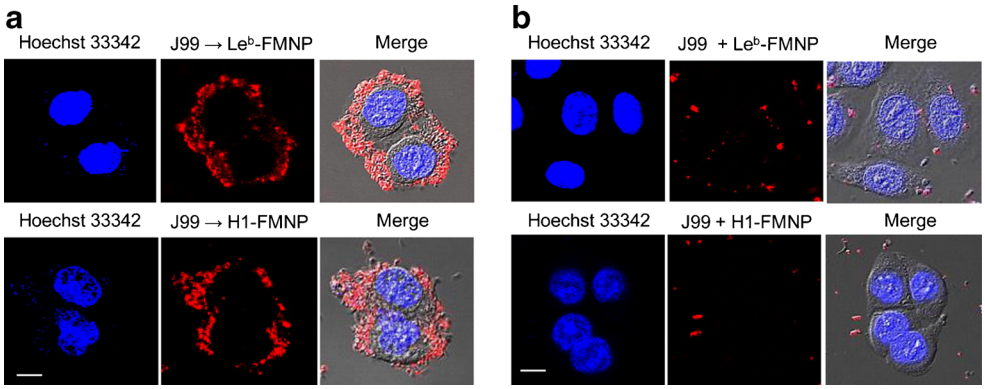

Fig. 12 GlycoMNP block adhesion of *Helicobacter pylori* J99 to mammalian cells. **a** AGS cells were incubated with *H. pylori* J99 for 0.5 h. J99 cells adhered to AGS cells were detected by treatment with fluorescent Lewis b (Le^b)-functionalized MNPs (*top*) and H1-functionalized MNPs (*bottom*) for 1 h. Cells were pretreated with Hoechst 33342 to stain the nucleus. **b** AGS cells, pretreated with Hoechst 33342, were incubated with *H. pylori* J99 for 0.5 h in the presence of Le^b-functionalized MNPs (*top*) and H1-functionalized MNPs (bottom). *Scale bar* 10 μm. *FMNP* functionalized MNP. (Reprinted with permission from [35], copyright 2015 American Chemical Society)

and *H. pylori* J99 for 30 min. By confocal microscopy it was possible to determine that most of the bacteria were not able to bind to the mammalian cells when the glycoMNPs were present (Fig. 12). Thus, these glycoMNPs could serve as a good platform to detect BabA-displaying pathogens, and at the same time, to block their adhesion to host cells.

Similar approaches have been used to detect and isolate DCs [43]. In an attempt to increase the low capture efficiency of currently available methods (mostly based on antibody-functionalized MNPs), Le^X was used to functionalize MNPs (Fig. 13, panel a). DC-specific intercellular adhesion molecule 3 grabbing nonintegrin (DC-SIGN), which is present on

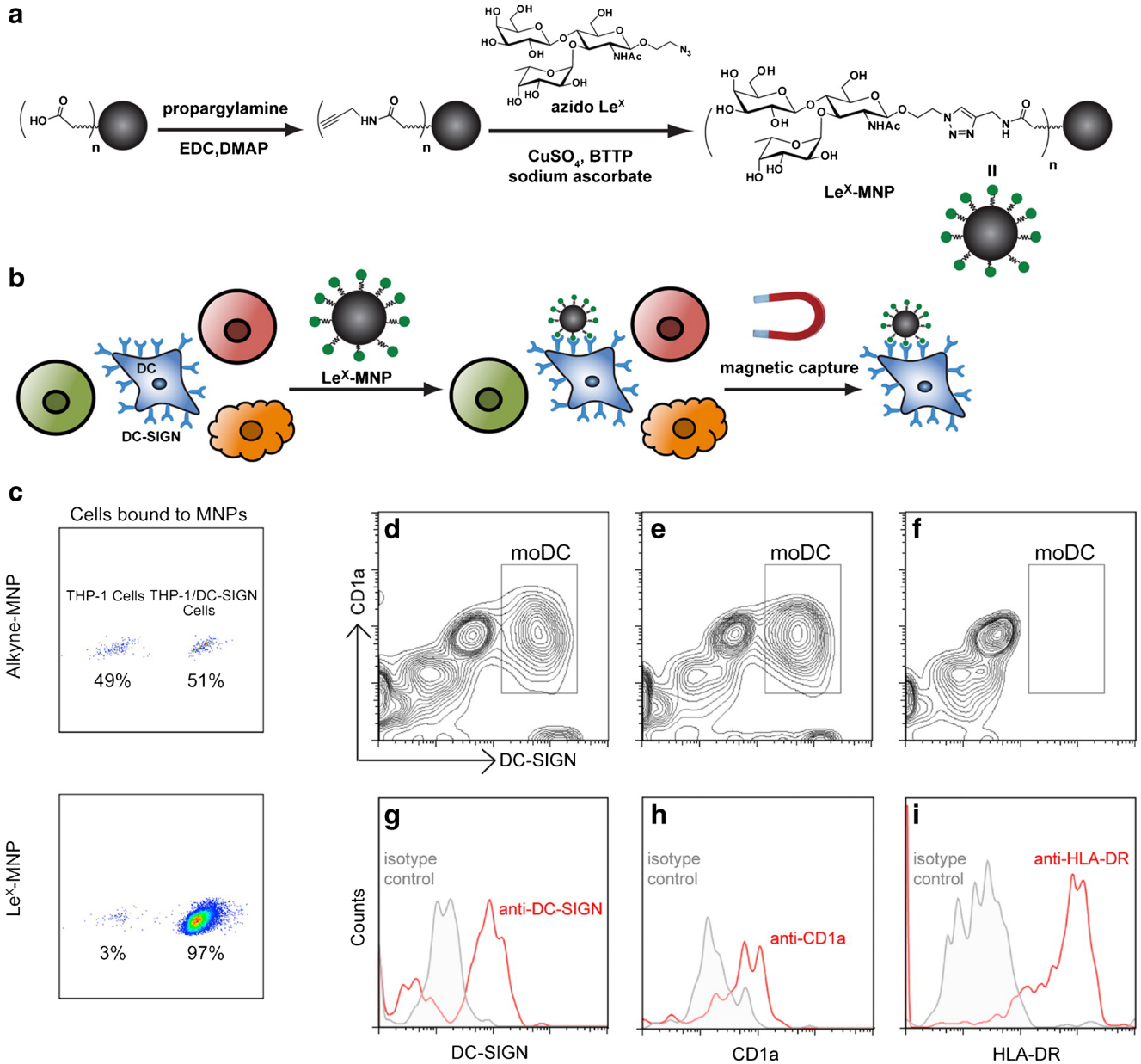

Fig. 13 *a* fabrication of Lewis X (Le^X)-functionalized MNPs (for details, see "Covalent functionalization with carbohydrates") and *b* selective capture of dendritic cells (*DC*) from a mixed cell population using Le^X-functionalized MNPs. *c* THP-1 DC-specific intercellular adhesion molecule 3 grabbing nonintegrin (*DC-SIGN*) cells were stained and mixed at a 1:1 ratio with unstained THP-1 cells. The cell mixture was incubated with different MNPs for 15 min and captured on a magnetic strip. The captured cells were analyzed by flow cytometry. The *numbers* shown in the *dot plots* represent the percentages of each cell type captured by the MNPs. Le^X-functionalized MNPs specifically bound to DC-SIGN-expressing cells and not to THP-1 cells, whereas control MNPs not bearing Le^X did not recognize any cells. *d* contour plot showing the total cell population before capture, where monocyte-derived DCs (*moDC*) were defined as $CD1a^+/DC\text{-}SIGN^+$ (gated in the *box*). *e* cell flow-through after incubation with alkyne-functionalized MNPs (control MNPs). *f* cell flow-through after incubation with Le^X-functionalized MNPs. *g–i* histograms show that the population of cells bound to Le^X-functionalized glycoMNPs were $CD1a^+/DC\text{-}SIGN^+/HLA\text{-}DR^+$. *BTTP* 3-(4-((bis((1-tertbutyl)-1*H*-1,2,3-triazol-4-yl)methyl)amino)methyl)-1*H*-1,2,3-triazol-1-yl)-propan-1-ol, *DMAP* 4-dimethylaminopyridine. (Adapted with permission from [43], copyright 2012 American Chemical Society)

immature and mature DCs, can recognize and bind these glycan epitopes. Therefore, the glycoMNPs could be used as a detection and cell enrichment tool (Fig. 13, panel b). The glycoMNPs were tested in a mixed cell population to assess their ability to capture DC-SIGN-positive cells (THP-1/DC-SIGN). After incubation with cultured cells, a magnetic field was applied to isolate the MNPs, and the cell populations were analysed by flow cytometry (Fig. 13, panel c). The capturing efficiency was approximately 70–86 %, much higher than that reported for commercially available antibody-functionalized MNPs used to isolate DCs (10−30 %) [43]. Importantly, incubation for 15 min was sufficient. To test if the glycoMNPs could be used to isolate primary DC-SIGN-expressing cells from a heterogeneous cell population, human monocytes were differentiated with use of growth factors. The method is useful to obtain monocyte-derived DCs (moDCs), but in most cases this population is mixed with undifferentiated monocytes. On incubation of the glycoMNPs with the growth-factor-treated cells, the cells bound to the glycoMNPs were separated from the unbound ones with a magnet and analysed by flow cytometry. Cells were stained with antibodies for moDC markers (DC-SIGN, CD1a and HLA-DR). The moDCs were completely captured from the heterologous cell population, as in the cell flow-through after incubation with the glycoMNPs, moDCs were not present (Fig. 13, panels d–f). On the other hand, cells isolated with use of the glycoMNPs were positive for the three markers (DC-SIGN, CD1a and HLA-DR) (Fig. 13, panels g–i).

Cell targeting

The attachment of carbohydrates to MNPs can be used to form glycoMNPs to selectively interact with cells, as carbohydrate-interacting proteins are major components of the surface of mammalian cells [70].

For instance, Kamat et al. [71] reported the use of hyaluronic acid (HA)-coated MNPs to target activated macrophages. As macrophages play an important role in infectious and inflammatory diseases, they are an excellent target for imaging or delivery of drugs. Since activated macrophages express specific receptors (CD44) that bind to HA, HA-coated MNPs are an excellent platform to actively target these macrophages. Results showed that HA-coated MNPs with an average size of 6 nm by transmission electron microscopy were rapidly taken up by activated THP-1 cells in vitro and that the uptake was dependent on the presence of HA and CD44.

To assess the role of different carbohydrates in cellular uptake, we synthesized 6-nm MNPs and functionalized them with glucose or galactose [33]. Both types of glycoMNPs were incubated with Vero (monkey kidney epithelial) cells for 15 min and observed by confocal microscopy. Although both glycoMNPs were taken up by the cells, the cellular distribution was different, with the glucose-functionalized MNPs distributed all over the cytoplasm and the galactose-functionalized MNPs remaining mainly in the cell periphery (Fig. 14a). The uptake kinetics was also different, as galactose-functionalized MNPs needed 4 h to be internalized, whereas glucose-functionalized MNPs were readily taken up after incubation for 15 min. Both glycoMNPs shared the same hydrodynamic size and *Z*potential, and differed only in the nature of the carbohydrate, suggesting therefore that slight changes in the monosaccharide can modify the cellular uptake of the MNPs. Use of different endocytosis inhibitors revealed that lipid rafts were preferentially involved in the cellular uptake of the glucose-functionalized MNPs. A high degree of colocalization with a lipid raft marker (cholera toxin) suggested that the caveolar route was the main mechanism involved in uptake of glucose-functionalized MNPs (Fig. 14b). Lysosome accumulation was demonstrated by live-imaging confocal microscopy using a marker for acidic compartments and lysosomes (Fig. 14c). Similar entrance patterns have been described for gold-coated iron oxide nanoparticles functionalized with lactose when incubated with a human cervical carcinoma cell line (C33) [30].

Apart from the nature of the carbohydrate [72], its spatial orientation can influence the cellular uptake. For instance, Lai et al. [39] reported the synthesis of 10-nm MNPs functionalized with a fluorescent dye and monoantennary or triantennary galactosyl ligands to selectively target liver cancer cells (HepG2) in vitro. These galactose residues can specifically interact with the extracellular ASGP-R, which is abundantly present in HepG2 cells, thus triggering the uptake of glycoMNPs into the cell. Incorporation of the fluorescent dye into the MNP produced a multimodal contrast agent, which could be used in MRI and fluorescence imaging to track cellular uptake. The specificity towards HepG2 cells was demonstrated by incubation of the same glycoMNPs with HeLa cells, which do not express ASGP-R. Receptor-mediated endocytosis of the glycoMNPs and lysosome accumulation by HepG2 cells was reported. More interestingly, the cellular uptake was different depending on the galactose residues, with the triantennary molecule 1a showing the best uptake efficiency owing to an optimal spatial orientation (see also "Covalent functionalization with carbohydrates" and Fig. 5 for the structures of the saccharides).

In another example, the incorporation of galactose onto the silica shell of MNPs led to their cellular uptake by A549 cells, probably mediated by lectins from the galectin family. As these proteins are present in the cytoplasm and nucleus of the cells, these glycoMNPs were also found in the nucleus of the cells, without exerting cytotoxic effects [44]. These differences in the final fate of MNPs coated with galactose (lysosomes versus cytoplasm and nucleus) can depend on many factors, such as the charge, size and hydrophobicity of the MNPs or the cell line used.

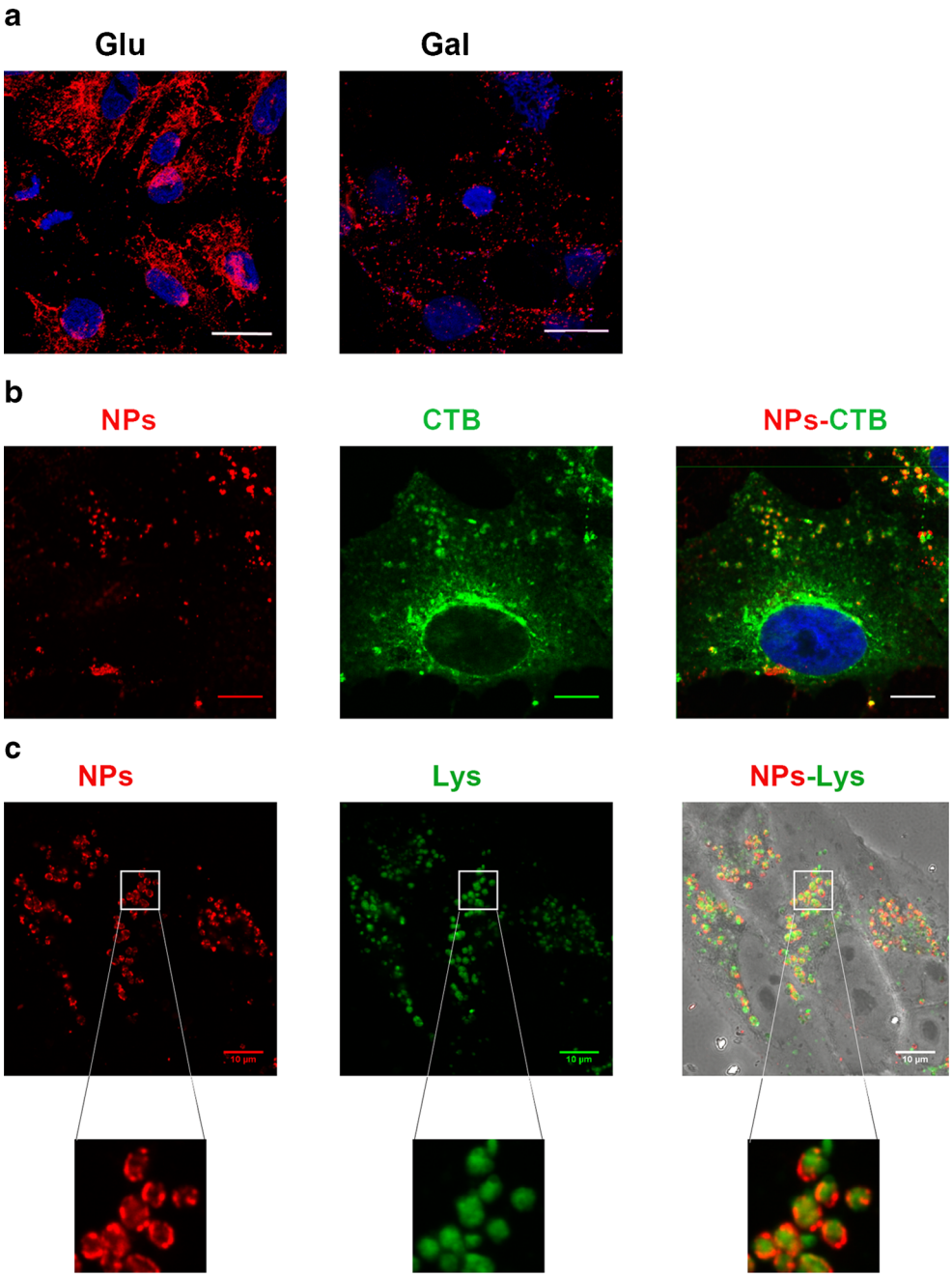

Fig. 14 **a** Confocal micrographs taken after 15 min of incubation of glucose-functionalized MNPs (*Glu*) and galactose-functionalized MNPs (*Gal*) in Vero cells. Glucose-functionalized MNPs were internalized in only 15 min, whereas galactose-functionalized MNPs remained mainly in the periphery. *Scale bar* 20 μm. **b** Cholera toxin colocalization with glucose-labelled MNPs analysed by confocal microscopy. Images from nanoparticles (*NPs*), cholera toxin labelled with Alexa Fluor 488 (*CTB*) and merged image (*NPs-CTB*), where a high degree of colocalization is observed. *Scale bar* 10 μm. **c** LysoTracker, a marker for acidic compartments was used to evaluate the possible accumulation of glucose-functionalized MNPs in lysosomes after incubation with cells for 2 h. Live-cell imaging was performed with a confocal microscope. Images from glucose-functionalized MNPs (*NPs*), LysoTracker (*Lys*), and merged channels (*NPs-Lys*) superimposed over the bright field image are shown. *Scale bar* 10 μm. (Adapted with permission from [33], copyright 2012 American Chemical Society)

Kavunja et al. [41] recently demonstrated the potential of galactose-functionalized MNPs for the isolation and characterization of lectins overexpressed in B16F10 metastatic melanoma cells. Galectin 3, a galactose-selective lectin, was isolated from the lysate of B16F10 cells after incubation with galactose-functionalized MNPs. Conversely, no lectin could be detected when mannose-functionalized MNPs or MNPs lacking the carbohydrate functionality were used. Importantly, this method could be extended to whole live cells with the aim to isolate known or unknown lectins from their native milieu. Proteomic analysis of the proteins bound to galactose-functionalized MNPs on their internalization by B16F10 cells revealed the successful isolation of serine/arginine-rich splicing factor 1 (SFRS1), annexin V and three histone proteins. SFRS1 is a glycan-binding protein overexpressed in B16F10 cells and has properties and cellular localization similar to those of galectin 1 and galectin 3, which are involved in metastatic growth. Therefore, SFRS1 could be a new target for cancer therapy and diagnosis. The fact that annexin and histone proteins could be co-isolated by galactose-functionalized MNPs was attributed to the formation of complexes of these proteins with SFRS1 and indicates the potential of glycoMNPs not only for the isolation and identification of lectins, but also for the study of their binding with other biomolecules.

Imaging

MRI is a non-invasive technique widely used in clinical diagnosis. It provides high contrast in soft tissue, three-dimensional information and spatial resolution of 20-50 μm for small animals [73]. In recent decades paramagnetic and superparamagnetic nanoparticles have been routinely used as contrast agents to improve the sensitivity of MRI [74]. Marradi et al. [75] reported the use of paramagnetic glyconanoparticles as T1-positive contrast agents, where gold nanoparticles were functionalized with different carbohydrates (glucose, galactose and lactose) and gadolinium complex derivatives. The longitudinal relaxivity (r1) values at 1.41 T were higher for galactose-functionalized and lactose-functionalized nanoparticles compared than for glucose-functionalized ones. These longitudinal relaxation values were almost six times higher than the values provided by Dotarem®, a contrast agent used clinically. In vivo, glucose-functionalized nanoparticles were able to reach the tumoral area in a mouse glioma model and to enhance the contrast in T1-weighted images, whereas lactose-functionalized ones did not reach the brain tumour, probably owing to enhanced liver uptake. Therefore, the nature of the carbohydrate can influence the relaxation of the water protons and the biodistribution of the nanoparticles in vivo. Although optimal T1-weighting properties have also been described for glycopeptide-stabilized superparamagnetic magnetite nanoparticles [42], most of the reports describe the use of iron oxide glycoMNPs as T2 contrast agents. The nature of the carbohydrate can also tune the transverse relaxivity (r2) values of iron oxide nanoparticles functionalized with rhamnose [24] or grafted with diblock copolymers bearing α-D-mannose, α-D-glucose or β-D-glucose [26]. In the latter, r2 relaxivity values at 9.4 T were higher for those MNPs bearing mannose than for the same MNPs functionalized with glucose. Further, r2 relaxivity values were higher for those MNPs functionalized with carbohydrates than for the MNPs grafted with only diblock copolymers. This is a consequence of the hydrophilicity of the MNP surface, which is enhanced when carbohydrates are present, as the transverse relaxivity depends on the diffusion of water molecules [76].

In vitro, glycoMNPs have been used in different fields, but mainly for selective labelling of cells. For instance, by incorporating a fluorescent dye into gold-coated MNPs, Gallo et al. [29] designed dual contrast agents that could be used to assess cellular labelling in blood. For the specific labelling of low-population peripheral blood mononuclear cells, glycoMNPs were functionalized with protein G in order to further incorporate in an oriented manner an anti-CD45 antibody to target leucocytes. Other glycoMNPs were designed with anti-CD235a to label erythrocytes. Both types of glycoMNPs were incubated with blood, and the specific labelling of peripheral blood mononuclear cells and red blood cells was demonstrated both by MRI and by fluorescence imaging.

In vivo MRI with glycoMNPs has been used to detect diseases [38], track the migration of endogenous neuronal stem cells in response to an induced tumour [31] or track stem cells [77]. For instance, unfractioned-heparin-coated superparamagnetic iron oxide nanoparticles were used to detect human mesenchymal stem cells, which are considered to be good candidates in regenerative medicine [77]. In vitro these glycoMNPs showed enhanced uptake by human mesenchymal stem cells when compared with dextran-coated MNPs and could be detected in the cells by Prussian blue staining for 28 days. More interestingly, if these cells were transplanted into nude mice, they could be detected by MRI even 1 month after transplantation (Fig. 15).

Presymptomatic in vivo imaging of early-activated cerebral endothelium was reported by van Kasteren et al. [38]. In this pioneering work, MNPs were functionalized with the glycan sLe^x in order to selectively target E-selectin and P-selectin, which play a relevant role in the homing of leucocytes to sites of inflammation. These glycoMNPs allowed direct detection of activated endothelium in a model of stroke in vivo by MRI, demonstrating high potential for early disease detection. A similar strategy was recently reported by Farr et al. [37], although the results differ slightly. Amino-functionalized silica iron oxide core–shell nanoparticles with a diameter of 18 nm were functionalized with sLe^X (SX@MNPs) to specifically target selectins, or Le^X (LX@MNP) as a control. The same MNPs without carbohydrates (OH-MNPs) were also used as a control. Results in vitro showed that, as expected, the binding specificity of the SX@MNPs for rat E-selectin was much higher than the binding specificity of both control MNPs. The three formulations were then administered to mice after they had undergone middle cerebral artery occlusion (MCAO), the commonest method to model transient stroke. The accumulation of MNPs was analysed by MRI acquiring $T2^*$-weighted images (Fig. 16, panels a–c). 24 h after MCAO, and it was found the SX@MNPs accumulated to a greater extent in the whole brain when compared with both control MNPs (Fig. 16, panel d). However, when the accumulation of MNPs was analysed as a ratio between the ischemic tissue and the corresponding mirrored region on the intact side of the brain, OH-MNPs appeared to have the highest ratio, whereas SX@MNPs had the lowest ratio (Fig. 16, panel e). Unexpectedly, in vivo, OH-MNPs accumulated in the ischemic zone to a greater extent than the glycoMNPs, which was opposed to the results found in vitro. By analysis of the selectin expression in the ischemic brain, it was found that selectins were upregulated throughout the entire brain and were not confined only to the injured tissue (Fig. 16, panel f). These results highlight the challenges that can arise when one changes from in vitro to in vivo work and the importance of working with appropriate control samples.

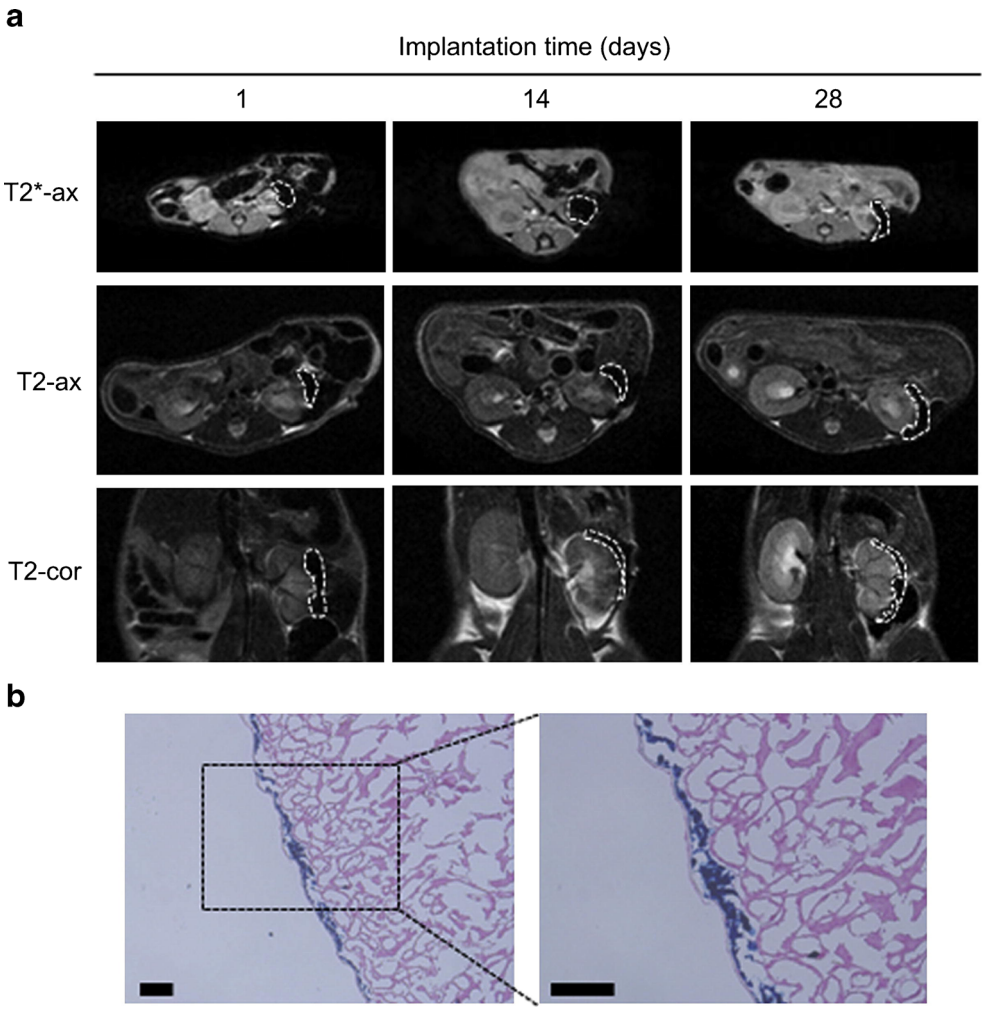

Fig. 15 **a** Axial and coronal images for the T2- and T2*-weighted magnetic resonance imaging of mice 28 days after the transplantation of unfractionated-heparin-coated superparamagnetic iron oxide (UFH-SPIO)-labelled human mesenchymal stem cells under the renal membrane. Transplanted regions are indicated by *white dashed lines*. **b** Histological staining results for UFH-SPIO-labelled human mesenchymal stem cells 28 days after transplantation. UFH-SPIO nanoparticles were stained with Prussian blue (*blue*) and counter stained with nuclear fast red (*pink*). The magnified image from the *black dotted rectangle* is shown on the *right*. *Scale bars* 100 mm. (Reprinted from [77], copyright 2012 with permission from Elsevier)

Perspectives and outlook

Over the past decade, glycoMNPs have demonstrated their usefulness for different biological applications, mainly in the fields of biosensing, magnetic separation and MRI. In this review we have given an overview of both the synthetic methods for constructing MNP glycoconjugates and their most promising bioapplications, focusing on relevant literature reports from the last 5 years.

In terms of sensing and separation applications, MNPs have shown clear advantages over other types of nanomaterials. For instance, assays based on MRS can be done with complex samples without requiring washing steps, and in some cases the sensitivity reported surpassed that of commercially available analysis systems. Surprisingly though, there are only a few examples of MRS sensing applications based on glycoMNPs, although many outstanding examples have been reported where MNPs functionalized with antibodies are used to detect and profile tumoral cells. GlycoMNPs are also excellent tools for separation and/or sample preconcentration purposes, as analytes of interest (including cells and bacteria) bound to glycoMNPs can be easily separated from complex mixtures by a magnet.

In the coming years, several challenges will have to be tackled by researchers working in the field of glycoMNPs. First, the chemistry needed to construct magnetic glycoconjugates is not as straightforward as the chemistry used, for instance, to construct gold glyconanoparticles (thiol–gold bond formation) [78]. The lack of a "universal" protocol to construct glycoMNPs, despite intense efforts to develop both successful covalent and successful non-covalent approaches for the preparation of glycoMNPs, could be the reason why the number of articles reporting the synthesis of glycoMNPs seems to be lower than in the case of gold glyconanoparticles. At this point, we stress once more the importance of the control of the surface density and presentation of carbohydrate ligands, which are both key for bioapplications of glycoMNPs.

As mentioned in "Introduction", MNPs are suitable for integration with miniaturized diagnostic systems. In this sense, perhaps the most promising approach is the micro NMR (μNMR), which has emerged as a novel sensing

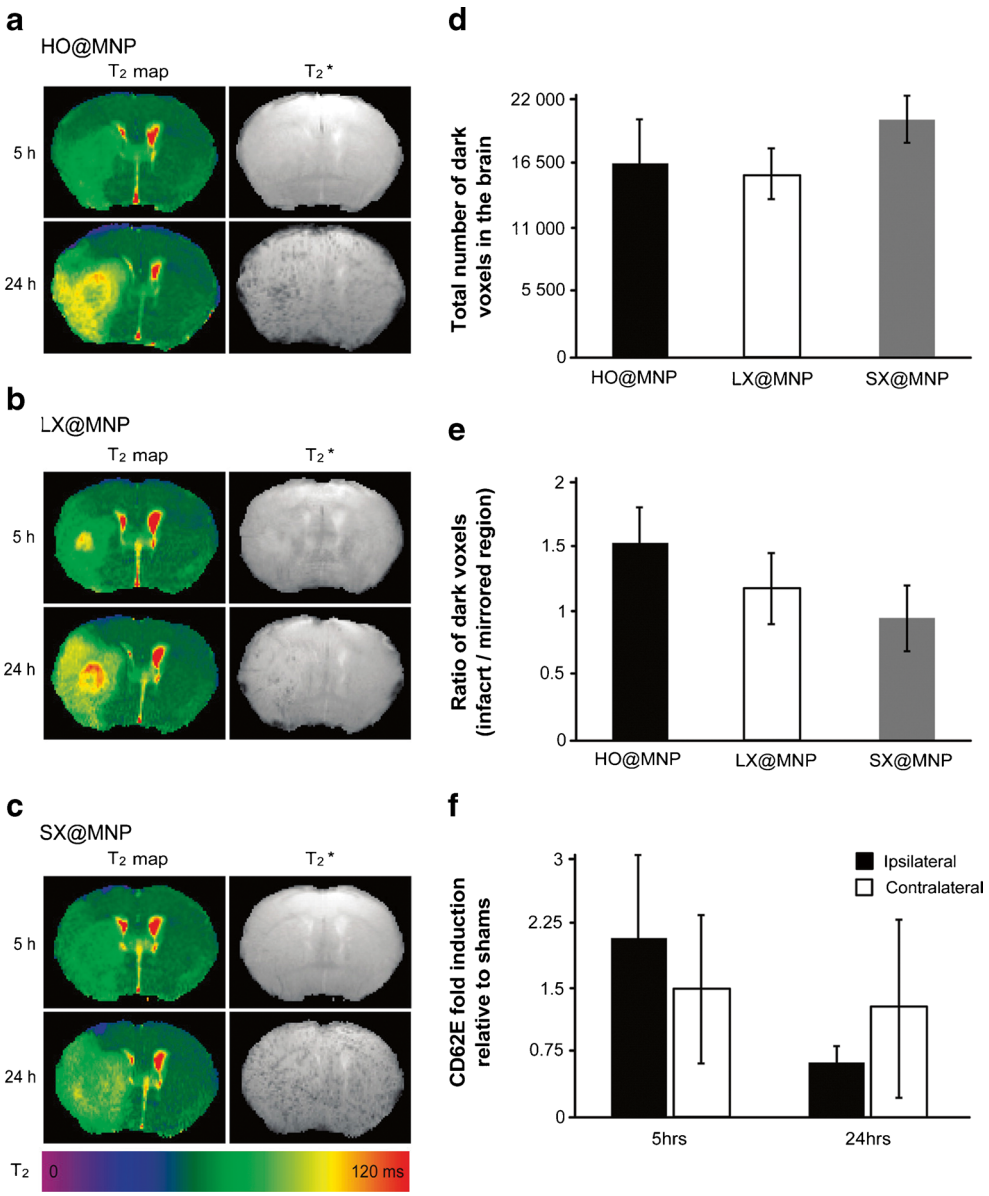

Fig. 16 T2 maps and T2*-weighted images at 5 and 24 h after middle cerebral artery occlusion (MCAO) in a mouse that received *a* amino-functionalized silica iron oxide core–shell nanoparticles with a diameter of 18 nm without carbohydrates (*HO@MNP*), *b* amino-functionalized silica iron oxide core–shell nanoparticles with a diameter of 18 nm functionalized with Lewis X (*LX@MNP*) or *c* amino-functionalized silica iron oxide core–shell nanoparticles with a diameter of 18 nm functionalized with sialyl Lewis X (*SX@MNP*). The *colour scale* corresponds to the T2 value (ms). *d* the total number of dark voxels in the brains of the mice from each group. *e* the number of dark voxels in the infarcted tissue expressed as a ratio of the mirrored contralateral region. *f* the amount of CD62E expression (in relation to sham animals) in the ipsilateral and contralateral hemispheres of mice with either 5 or 24 h of MCAO. Not significant differences in the expression were found. (Adapted with permission from [37], copyright 2014 American Chemical Society)

technology for detection of biomarkers and circulating tumour cells using portable miniaturized NMR systems (for a comprehensive review of μNMR, including its translational aspects towards clinical applications, see [55]). Despite several successful applications of μNMR sensing with MNPs functionalized with antibodies, no examples involving glycoMNPs have been reported in the literature so far. Some hurdles associated with this include the difficulty to achieve controlled synthesis of complex oligosaccharides, whereas antibodies can be produced against almost every antigen, ranging from large ones (bacteria, viruses, etc.) to small ones (hormones, drugs, etc.). Apart from their diversity, antibodies show high specificity and binding affinity for their target molecules, making them ideal candidates for functionalization of MNPs. Antibodies, on the other hand, have a complex three-dimensional structure, and the orientation on the surface of the MNP is crucial to attain high sensitivity in biosensing applications. Carbohydrates are less prone to denaturation than antibodies and also have high specificity; therefore, their conjugation onto the surface of MNPs in an easier way could be an interesting alternative. Given the potential of glycoMNPs to detect carbohydrate-binding proteins characteristic of different types of cancer cells, the integration with miniaturized NMR systems could be one of the most active research areas in the field of biosensing using glycoMNPs.

Another important challenge is related to the translation from in vitro to in vivo studies. As highlighted in some of the examples discussed here, contradictory results can be obtained when one moves to in vivo work, and researchers should take into account not only the appropriate

biofunctionalization of the MNPs, but also the complexity of the in vivo scenario. Nevertheless, there could be important advances in the coming years in the field of in vivo applications of glycoMNPs. The most promising applications, in our opinion, will arise in the field of imaging, where the advantage of active targeting through carbohydrate ligands could be combined with the intrinsic ability of MNPs to act as MRI contrast agents.

Acknowledgments This work was funded by European Research Council Starting Grant 239931-NANOPUZZLE. J.M.F. acknowledges the SAF2014-54763-C2-2-R project (Spanish Government), European Regional and Social Development Funds, and the Aragón Autonomous Government (DGA) through Research Groups. R.M.F. acknowledges the University of Zaragoza and ARAID for financial support.

Conflict of interest The authors declare that they have no conflict of interest.

References

1. Adak AK, Li B-Y, Lin C-C (2015) Advances in multifunctional glycosylated nanomaterials: preparation and applications in glycoscience. Carbohydr Res 405:2–12
2. Gamblin DP, Scanlan EM, Davis BG (2009) Glycoprotein synthesis: an update. Chem Rev 109:131–163
3. Dennis JW, Granovsky M, Warren CE (1999) Glycoprotein glycosylation and cancer progression. Biochim Biophys Acta 1473:21–34
4. Cipolla L, Peri F (2011) Carbohydrate-based bioactive compounds for medicinal chemistry applications. Mini Rev Med Chem 11:39–54
5. Reis CA, Osorio H, Silva L, Gomes C, David L (2010) Alterations in glycosylation as biomarkers for cancer detection. J Clin Pathol 63:322–329
6. Stowell SR, Ju T, Cummings RD (2015) Protein glycosylation in cancer. Annu Rev Pathol Mech Dis 10:473–510
7. Johnson JL, Jones MB, Ryan SO, Cobb BA (2013) The regulatory power of glycans and their binding partners in immunity. Trends Immunol 34:290–298
8. De la Fuente JM, Penadés S (2006) Glyconanoparticles: types, synthesis and applications in glycoscience, biomedicine and material science. Biochim Biophys Acta 1760:636–651
9. Marradi M, Chiodo F, García I, Penadés S (2013) Glyconanoparticles as multifunctional and multimodal carbohydrate systems. Chem Soc Rev 42:4728–4745
10. Lee N, Hyeon T (2012) Designed synthesis of uniformly sized iron oxide nanoparticles for efficient magnetic resonance imaging contrast agents. Chem Soc Rev 41:2575
11. Kumar CSSR, Mohammad F (2011) Magnetic nanomaterials for hyperthermia-based therapy and controlled drug delivery. Adv Drug Deliv Rev 63:789–808
12. Kievit FM, Zhang M (2011) Surface engineering of iron oxide nanoparticles for targeted cancer therapy. Acc Chem Res 44:853
13. Veiseh O, Gunn JW, Zhang M (2010) Design and fabrication of magnetic nanoparticles for targeted drug delivery and imaging. Adv Drug Deliv Rev 62:284
14. Colombo M, Carregal-Romero S, Casula MF, Gutiérrez L, Morales MP, Böhm IB, Heverhagen JT, Prosperi D, Parak WJ (2012) Biological applications of magnetic nanoparticles. Chem Soc Rev 41:4306
15. Rocha-Santos TAP (2014) Sensors and biosensors based on magnetic nanoparticles. Trends Anal Chem 62:28–36
16. Issadore D, Park YI, Shao H, Min C, Lee K, Liong M, Weissleder R, Lee H (2014) Magnetic sensing technology for molecular analyses. Lab Chip 14:2385
17. Tassa C, Duffner JL, Lewis TA, Weissleder R, Schreiber SL, Koehler AN, Shaw SY (2010) Binding affinity and kinetic analysis of targeted small molecule-modified nanoparticles. Bioconjug Chem 21:14–19
18. Barrientos AG, de la Fuente JM, Jiménez M, Solís D, Cañada FJ, Martín-Lomas M, Penadés S (2009) Modulating glycosidase degradation and lectin recognition of gold glyconanoparticles. Carbohydr Res 344:1474–1478
19. Moros M, Pelaz B, López-Larrubia P, García-Martin ML, Grazú V, de la Fuente JM (2010) Engineering biofunctional magnetic nanoparticles for biotechnological applications. Nanoscale 2:1746–1755
20. Horák D, Babič M, Jendelová P, Herynek V, Trchová M, Pientka Z, Pollert E, Hájek M, Syková E (2007) D-Mannose-modified iron oxide nanoparticles for stem cell labeling. Bioconjug Chem 18:635–644
21. Kekkonen V, Lafreniere N, Ebara M, Saito A, Sawa Y, Narain R (2009) Synthesis and characterization of biocompatible magnetic glyconanoparticles. J Magn Magn Mater 321:1393–1396
22. Baccile N, Noiville R, Stievano L, Van Bogaert I (2013) Sophorolipids-functionalized iron oxide nanoparticles. Phys Chem Chem Phys 15:1606–1620
23. Lartigue L, Oumzil K, Guari Y, Larionova J, Guérin C, Montero J-L, Barragan-Montero V, Sangregorio C, Caneschi A, Innocenti C, Kalaivani T, Arosio P, Lascialfari A (2009) Water-soluble rhamnose-coated Fe_3O_4 nanoparticles. Org Lett 11:2007–2010
24. Lartigue L, Innocenti C, Kalaivani T, Awwad A, Sanchez Duque MDM, Guari Y, Larionova J, Guérin C, Montero JLG, Barragan-Montero V, Arosio P, Lascialfari A, Gatteschi D, Sangregorio C (2011) Water-dispersible sugar-coated iron oxide nanoparticles. An evaluation of their relaxometric and magnetic hyperthermia properties. J Am Chem Soc 133:10459–10472
25. Nativi C, Manuelli M, Richichi B, Sangregorio C, Lombardi G, Fallarini S (2014) Iron oxide superparamagnetic nanoparticles conjugated with a conformationally blocked α-Tn antigen mimetic for macrophage activation. Nanoscale 6:7643–7655
26. Basuki JS, Esser L, Duong HTT, Zhang Q, Wilson P, Whittaker MR, Haddleton DM, Boyer C, Davis TP (2014) Magnetic nanoparticles with diblock glycopolymer shells give lectin concentration-dependent MRI signals and selective cell uptake. Chem Sci 5:715
27. Gallo J, García I, Padro D, Arnáiz B, Penadés S (2010) Water-soluble magnetic glyconanoparticles based on metal-doped ferrites coated with gold: synthesis and characterization. J Mater Chem 20:10010
28. García I, Gallo J, Genicio N, Padro D, Penadés S (2011) Magnetic glyconanoparticles as a versatile platform for selective immunolabeling and imaging of cells. Bioconjug Chem 22:264–273
29. Gallo J, García I, Genicio N, Padro D, Penadés S (2011) Specific labelling of cell populations in blood with targeted immuno-fluorescent/magnetic glyconanoparticles. Biomaterials 32:9818–9825
30. Gallo J, Genicio N, Penadés S (2012) Uptake and intracellular fate of fluorescent-magnetic glyco-nanoparticles. Adv Healthcare Mater 1:302–307
31. Elvira G, García I, Benito M, Gallo J, Desco M, Penadés S, Garcia-Sanz JA, Silva A (2012) Live imaging of mouse endogenous neural progenitors migrating in response to an induced tumor. PLoS One 7:e44466
32. Elvira G, García I, Gallo J, Benito M, Montesinos P, Holgado-Martin E, Ayuso-Sacido A, Penadés S, Desco M, Silva A, Garcia-Sanz JA (2015) Detection of mouse endogenous type B astrocytes migrating towards brain lesions. Stem Cell Res 14:114–129

33. Moros M, Hernáez B, Garet E, Dias JT, Sáez B, Grazú V, González-Fernández Á, Alonso C, De La Fuente JM (2012) Monosaccharides versus PEG-functionalized NPs: influence in the cellular uptake. ACS Nano 6:1565–1577
34. Salado J, Insausti M, Lezama L, Gil de Muro I, Moros M, Pelaz B, Grazu V, de la Fuente JM, Rojo T (2012) Functionalized Fe_3O_4@Au superparamagnetic nanoparticles: in vitro bioactivity. Nanotechnology 23:315102
35. Park S, Kim G-H, Park S-H, Pai J, Rathwell D, Park J-Y, Kang Y-S, Shin I (2015) Probing cell-surface carbohydrate binding proteins with dual-modal glycan-conjugated nanoparticles. J Am Chem Soc 137:5961–5968
36. Kouyoumdjian H, Zhu DC, El-Dakdouki MH, Lorenz K, Chen J, Li W, Huang X (2013) Glyconanoparticle aided detection of β-amyloid by magnetic resonance imaging and attenuation of β-amyloid induced cytotoxicity. ACS Chem Neurosci 4:575–584
37. Farr TD, Lai C-H, Grünstein D, Orts-Gil G, Wang C-C, Boehm-Sturm P, Seeberger PH, Harms C (2014) Imaging early endothelial inflammation following stroke by core shell silica superparamagnetic glyconanoparticles that target selectin. Nano Lett 14:2130–2134
38. van Kasteren SI, Campbell SJ, Serres S, Anthony DC, Sibson NR, Davis BG (2009) Glyconanoparticles allow pre-symptomatic in vivo imaging of brain disease. Proc Natl Acad Sci U S A 106: 18–23
39. Lai CH, Lin CY, Wu HT, Chan HS, Chuang YJ, Chen CT, Lin CC (2010) Galactose encapsulated multifunctional nanoparticle for HepG2 cell internalization. Adv Funct Mater 20:3948–3958
40. El-Boubbou K, Zhu DC, Vasileiou C, Borhan B, Prosperi D, Li W, Huang X (2010) Magnetic glyco-nanoparticles: a tool to detect, differentiate, and unlock the glyco-codes of cancer via magnetic resonance imaging. J Am Chem Soc 132:4490–4499
41. Kavunja HW, Voss PG, Wang JL, Huang X (2015) Identification of lectins from metastatic cancer cells through magnetic glyconanoparticles. Isr J Chem 55:423–436
42. Borase T, Ninjbadgar T, Kapetanakis A, Roche S, O'Connor R, Kerskens C, Heise A, Brougham DF (2013) Stable aqueous dispersions of glycopeptide-grafted selectably functionalized magnetic nanoparticles. Angew Chem Int Ed 52:3164–3167
43. Rouhanifard SH, Xie R, Zhang G, Sun X, Chen X, Wu P (2012) Detection and isolation of dendritic cells using Lewis X-functionalized magnetic nanoparticles. Biomacromolecules 13: 3039–3045
44. Pfaff A, Schallon A, Ruhland TM, Majewski AP, Schmalz H, Freitag R, Müller AHE (2011) Magnetic and fluorescent glycopolymer hybrid nanoparticles for intranuclear optical imaging. Biomacromolecules 12:3805–3811
45. Liu LH, Dietsch H, Schurtenberger P, Yan M (2009) Photoinitiated coupling of unmodified monosaccharides to iron oxide nanoparticles for sensing proteins and bacteria. Bioconjug Chem 20:1349–1355
46. Jayawardena HSN, Jayawardana KW, Chen X, Yan M (2013) Maltoheptaose promotes nanoparticle internalization by Escherichia coli. Chem Commun 49:3034–3036
47. Kulkarni AA, Weiss AA, Iyer SS (2010) Detection of carbohydrate binding proteins using magnetic relaxation switches. Anal Chem 82:7430–7435
48. Parera Pera N, Kouki A, Haataja S, Branderhorst HM, Liskamp RMJ, Visser GM, Finne J, Pieters RJ (2010) Detection of pathogenic Streptococcus suis bacteria using magnetic glycoparticles. Org Biomol Chem 8:2425–2429
49. Chien WT, Yu CC, Liang CF, Lai CH, Lin PC, Lin CC (2011) Functionalized glyconanoparticles for the study of glycobiology. ACS Symp Ser 1091:15–36
50. Chen X, Ramström O, Yan M (2014) Glyconanomaterials: emerging applications in biomedical research. Nano Res 7:1381–1403
51. El-Boubbou K, Huang X (2011) Glyco-nanomaterials: translating insights from the "sugar-code" to biomedical applications. Curr Med Chem 18:2060–2078
52. Krishnan KM, Pakhomov AB, Bao Y, Blomqvist P, Chun Y, Gonzales M, Griffin K, Ji X, Roberts BK (2006) Nanomagnetism and spin electronics: materials, microstructure and novel properties. J Mater Sci 41:793–815
53. Pöselt E, Kloust H, Tromsdorf U, Janschel M, Hahn C, Maßlo C, Weller H (2012) Relaxivity optimization of a pegylated iron-oxide-based negative magnetic resonance contrast agent for T2-weighted spin-echo imaging. ACS Nano 6:1619–1624
54. De M, Chou SS, Joshi HM, Dravid VP (2011) Hybrid magnetic nanostructures (MNS) for magnetic resonance imaging applications. Adv Drug Deliv Rev 63:1282–1299
55. Castro CM, Ghazani AA, Chung J, Shao H, Issadore D, Yoon T-J, Weissleder R, Lee H (2014) Miniaturized nuclear magnetic resonance platform for detection and profiling of circulating tumor cells. Lab Chip 14:14–23
56. Kaittanis C, Santra S, Perez JM (2009) Role of nanoparticle valency in the nondestructive magnetic-relaxation-mediated detection and magnetic isolation of cells in complex media. J Am Chem Soc 131: 12780–12791
57. Demas V, Lowery TJ (2011) Magnetic resonance for in vitro medical diagnostics: superparamagnetic nanoparticle-based magnetic relaxation switches. New J Phys 13:025005
58. Chen YP, Zou MQ, Qi C, Xie MX, Wang DN, Wang YF, Xue Q, Li JF, Chen Y (2013) Immunosensor based on magnetic relaxation switch and biotin-streptavidin system for the detection of kanamycin in milk. Biosens Bioelectron 39:112–117
59. Sun EY, Weissleder R, Josephson L (2006) Continuous analyte sensing with magnetic nanoswitches. Small 2:1144–1147
60. Köber M, Moros M, Franco Fraguas L, Grazú V, de la Fuente JM, Luna M, Briones F (2014) Nanoparticle-mediated monitoring of carbohydrate–lectin interactions using transient magnetic birefringence. Anal Chem 86:12159–12165
61. Chuang Y-J, Zhou X, Pan Z, Turchi C (2009) A convenient method for synthesis of glyconanoparticles for colorimetric measuring carbohydrate-protein interactions. Biochem Biophys Res Commun 389:22–27
62. Liang C-H, Wang C-C, Lin Y-C, Chen C-H, Wong C-H, Wu C-Y (2009) Iron oxide/gold core/shell nanoparticles for ultrasensitive detection of carbohydrate-protein interactions. Anal Chem 81: 7750–7756
63. Weatherman RV, Mortell KH, Chervenak M, Kiessling LL, Toone EJ (1996) Specificity of C-glycoside complexation by mannose/glucose specific lectins. J Biochem 35:3619–3624
64. Cai S, Liang G, Zhang P, Chen H, Zhang S, Liu B, Kong J (2011) Rational strategy of magnetic relaxation switches for glycoprotein sensing. Analyst 136:201–204
65. Parera Pera N, Pieters RJ (2014) Towards bacterial adhesion-based therapeutics and detection methods. Med Chem Commun 5:1027–1035
66. El-Boubbou K, Gruden C, Huang X (2007) Magnetic glyco-nanoparticles: A unique tool for rapid pathogen detection, decontamination, and strain differentiation. J Am Chem Soc 129:13392–13393
67. Hatch DM, Weiss AA, Kale RR, Iyer SS (2008) Biotinylated bi- and tetra-antennary glycoconjugates for Escherichia coli detection. ChemBioChem 9:2433–2442
68. Lin PC, Yu CC, Wu HT, Lu YW, Han CL, Su AK, Chen YJ, Lin CC (2013) A chemically functionalized magnetic nanoplatform for rapid and specific biomolecular recognition and separation. Biomacromolecules 14:160–168
69. Behra M, Azzouz N, Schmidt S, Volodkin DV, Mosca S, Chanana M, Seeberger PH, Hartmann L (2013) Magnetic porous sugar-functionalized PEG microgels for efficient isolation and removal of bacteria from solution. Biomacromolecules 14:1927–1935

70. Yilmaz G, Becer CR (2015) Glyconanoparticles and their interactions with lectins. Polym Chem 6:5503–5514. doi:10.1039/C5PY00089K
71. Kamat M, El-Boubbou K, Zhu DC, Lansdell T, Lu X, Li W, Huang X (2010) Hyaluronic acid immobilized magnetic nanoparticles for active targeting and imaging of macrophages. Bioconjug Chem 21: 2128–2135
72. de la Fuente JM, Alcántara D, Penadés S (2007) Cell response to magnetic glyconanoparticles: does the carbohydrate matter? IEEE Trans Nanobiosci 6:275–781
73. Bennett KM, Jo J-I, Cabral H, Rumiana B, Aoki I (2014) MR imaging techniques for nano-pathophysiology. Adv Drug Deliv Rev 74:75–94
74. Shokrollahi H (2013) Contrast agents for MRI. Mater Sci Eng C 33: 4485–4497
75. Marradi M, Alcántara D, de la Fuente JM, García-Martín ML, Cerdán S, Penadés S (2009) Paramagnetic Gd-based gold glyconanoparticles as probes for MRI: tuning relaxivities with sugars. Chem Commun 3922–3924
76. Carroll MRJ, Huffstetler PP, Miles WC, Goff JD, Davis RM, Riffle JS, House MJ, Woodward RC, St Pierre TG (2011) The effect of polymer coatings on proton transverse relaxivities of aqueous suspensions of magnetic nanoparticles. Nanotechnology 22:325702
77. Lee J-H, Jung MJ, Hwang YH, Lee YJ, Lee S, Lee DY, Shin H (2012) Heparin-coated superparamagnetic iron oxide for in vivo MR imaging of human MSCs. Biomaterials 33:4861–4871
78. De La Fuente JM, Alcántara D, Eaton P, Crespo P, Rojas TC, Fernández A, Hernando A, Penadés S (2006) Gold and gold-iron oxide magnetic glyconanoparticles: synthesis, characterization and magnetic properties. J Phys Chem B 110:13021–13028